

University of Dundee

Antikinetoplastid SAR study in 3-nitroimidazopyridine series

Fersing, Cyril; Boudot, Clotilde; Paoli-Lombardo, Romain; Primas, Nicolas; Pinault, Emilie; Hutter, Sébastien

Published in:
European Journal of Medicinal Chemistry

DOI:
[10.1016/j.ejmech.2020.112668](https://doi.org/10.1016/j.ejmech.2020.112668)

Publication date:
2020

Licence:
CC BY-NC-ND

Document Version
Peer reviewed version

[Link to publication in Discovery Research Portal](#)

Citation for published version (APA):

Fersing, C., Boudot, C., Paoli-Lombardo, R., Primas, N., Pinault, E., Hutter, S., Castera-Ducros, C., Kabri, Y., Pedron, J., Bourgeade-Delmas, S., Sournia-Saquet, A., Stigliani, J. L., Valentin, A., Azqueta, A., Muruzabal, D., Destere, A., Wyllie, S., Fairlamb, A. H., Corvaisier, S., ... Verhaeghe, P. (2020). Antikinetoplastid SAR study in 3-nitroimidazopyridine series: identification of a novel non-genotoxic and potent anti-T. b. brucei hit-compound with improved pharmacokinetic properties. *European Journal of Medicinal Chemistry*, 206, [112668]. <https://doi.org/10.1016/j.ejmech.2020.112668>

General rights

Copyright and moral rights for the publications made accessible in Discovery Research Portal are retained by the authors and/or other copyright owners and it is a condition of accessing publications that users recognise and abide by the legal requirements associated with these rights.

- Users may download and print one copy of any publication from Discovery Research Portal for the purpose of private study or research.
- You may not further distribute the material or use it for any profit-making activity or commercial gain.
- You may freely distribute the URL identifying the publication in the public portal.

Take down policy

If you believe that this document breaches copyright please contact us providing details, and we will remove access to the work immediately and investigate your claim.

Antikinetoplastid SAR study in 3-nitroimidazopyridine series: identification of a novel non-genotoxic and potent anti-*T. b. brucei* hit-compound with improved pharmacokinetic properties.

Cyril Fersing^{1#}, Clotilde Boudot^{2#}, Romain Paoli-Lombardo¹, Nicolas Primas¹, Emilie Pinault³, Sébastien Hutter⁴, Caroline Castera-Ducros¹, Youssef Kabri¹, Julien Pedron⁵, Sandra Bourgeade-Delmas⁶, Alix Sournia-Saquet⁵, Jean-Luc Stigliani⁵, Alexis Valentin⁶, Amaya Azqueta⁷, Damián Muruzabal⁷, Alexandre Destere⁸, Susan Wyllie⁹, Alan H. Fairlamb⁹, Sophie Corvaisier¹⁰, Marc Since¹⁰, Aurélie Malzert-Fréon¹⁰, Carole Di Giorgio¹¹, Pascal Rathelot¹, Nadine Azas⁴, Bertrand Courtioux², Patrice Vanelle¹ and Pierre Verhaeghe^{5*}.

¹ Aix Marseille Univ, CNRS, ICR UMR 7273, Equipe Pharmaco-Chimie Radicalaire, Faculté de Pharmacie, 27 Boulevard Jean Moulin, CS30064, 13385, Marseille Cedex 05, France.

² Université de Limoges, UMR Inserm 1094, Neuroépidémiologie Tropicale, Faculté de Pharmacie, 2 rue du Dr Marcland, 87025 Limoges, France.

³ Université de Limoges, BISCEM, US 042 INSERM – UMS 2015 CNRS, Mass Spectrometry Platform, CBRS, 2 rue du Pr. Descottes, F-87025 Limoges, France.

⁴ Aix Marseille Univ, IHU Méditerranée Infection, UMR VITROME - Tropical Eukaryotic Pathogens, 19-21 Boulevard Jean Moulin, 13005 Marseille, France.

⁵ LCC-CNRS Université de Toulouse, CNRS, UPS, Toulouse, France.

⁶ UMR 152 PHARMA-DEV, Université de Toulouse, IRD, UPS, Toulouse, France.

⁷ Department of Pharmacology and Toxicology, Faculty of Pharmacy and Nutrition, University of Navarra, C/ Irunlarrea 1, CP 31008, Pamplona, Navarra, Spain.

⁸ Department of Pharmacology, Toxicology and Pharmacovigilance, CHU Limoges, Limoges, France, INSERM, UMR 1248, University of Limoges, France.

⁹ University of Dundee, School of Life Sciences, Division of Biological Chemistry and Drug Discovery, Dow Street, Dundee DD1 5EH, Scotland, United Kingdom.

¹⁰ Normandie Univ, UNICAEN, CERMN, 14000 Caen, France.

¹¹ Institut Méditerranéen de Biodiversité et d'Ecologie marine et continentale (IMBE), Aix-Marseille Université, UMR CNRS IRD Avignon Université, Campus Timone – Faculté de Pharmacie, 27 boulevard Jean-Moulin, F13385 Marseille cedex 05.

#Co first-authors

*Corresponding author:

E-mail address: pierre.verhaeghe@lcc-toulouse.fr (P. Verhaeghe)

Postal address: Université Paul Sabatier - CNRS UPR 8241, Laboratoire de Chimie de Coordination, 205 Route de Narbonne, 31077 Toulouse cedex 04, France.

Abstract:

To study the antikinoplastid 3-nitroimidazo[1,2-*a*]pyridine pharmacophore, a structure-activity relationship study was conducted through the synthesis of 26 original derivatives and their *in vitro* evaluation on both *Leishmania spp* and *Trypanosoma brucei brucei*. This SAR study showed that the antitrypanosomal pharmacophore was less restrictive than the antileishmanial one and highlighted positions 2, 6 and 8 of the imidazopyridine ring as key modulation points. None of the synthesized compounds allowed improvement in antileishmanial activity, compared to previous hit molecules in the series. Nevertheless, compound **8**, the best antitrypanosomal molecule in this series ($EC_{50} = 17 \text{ nM}$, $SI = 2650$ & $E^{\circ} = -0.6 \text{ V}$), was not only more active than all reference drugs and previous hit molecules in the series but also displayed improved aqueous solubility and better *in vitro* pharmacokinetic characteristics: good microsomal stability ($T_{1/2} > 40 \text{ min}$), moderate albumin binding (77 %) and moderate permeability across the blood brain barrier according to a PAMPA assay. Moreover, both micronucleus and comet assays showed that nitroaromatic molecule **8** was not genotoxic *in vitro*. It was evidenced that bioactivation of molecule **8** was operated by *T. b. brucei* type 1 nitroreductase, in the same manner as fexinidazole. Finally, a mouse pharmacokinetic study showed that **8** displayed good systemic exposure after both single and repeated oral administrations at 100 mg/kg (NOAEL) and satisfying plasmatic half-life ($T_{1/2} = 7.7 \text{ h}$). Thus, molecule **8** appears as a good candidate for initiating a hit to lead drug discovery program.

Keywords: Imidazo[1,2-*a*]pyridine; Nitroaromatic; Nitroreductases; Kinetoplastids; Redox potentials; SARs.

1. Introduction

Kinetoplastid diseases are vectorial parasitoses caused by flagellated blood protozoa and transmitted to their hosts by specific insect vectors. These diseases are found in developing countries in intertropical regions, especially where health facilities are inadequate [1]. They threaten nearly one billion people, causing an estimated 30 000 deaths annually [2]. The World Health Organization (WHO) thereby classifies them as Neglected Tropical Diseases (NTDs) [3]. These infectious diseases are caused by two parasitic genera: *Leishmania* spp. and *Trypanosoma* spp. The first is responsible for leishmaniasis (caused by several *Leishmania* species) which can evolve in different forms (visceral, cutaneous or cutaneomucous) [4].

The second genus contains most of *Trypanosoma* species especially *T. cruzi* causing Chagas disease in South and Central America, and *T. brucei* spp. responsible for Human African Trypanosomiasis (HAT, or sleeping sickness) [5,6]. HAT is found in 36 countries throughout sub-Saharan Africa. It is estimated that 70 million people would be at risk of contracting it [7]. Two subspecies, *T. brucei gambiense* (*T.b.g.*) and *T. brucei rhodesiense* (*T.b.r.*), are at the origin of different symptoms and two clinical forms: chronic disease for *T.b.g.* and acute disease for *T.b.r.* Following the bite of the blood sucking fly (tsetse fly or glossina), the parasite penetrates into the derma and disseminates into the whole organism. In a first step, blood and lymph are affected by the bloodstream form, and patients show headaches, anemia, joint pain and various organ damages occur. This stage is called hemolymphatic stage. Then, without treatment, the parasites are able to cross the blood brain barrier (BBB) and invade the central nervous system (stage 2, or nervous stage), causing various neurological changes such as sleeping disorders (responsible for the name of the disease), abnormal tone and mobility, ataxia, psychiatric disorders, seizures, coma and finally, death, as all kinetoplastid diseases are lethal if untreated [7,8]. Nevertheless, very few efficient, safe and affordable drugs are proposed to treat the infected populations. Regarding HAT, treatments are complex because they are stage and species dependent. For early stage HAT, suramin and pentamidine, molecules presenting severe side effects, must be given by injection (IV

or IM) for a prolonged period against *T.b.r.* and *T.b.g.* infections, respectively. For the late-stage, melarsoprol is given in *T.b.r.* infections despite the high toxicity of this arsenic derivative (it can cause encephalopathies in 10% of cases). Against *T.b.g.* infections, the NECT (Nifurtimox Eflornithine Combination Therapy) is prescribed despite the genotoxic character of nifurtimox [9]. Since the end of 2018, a new safer nitroaromatic drug, fexinidazole, is available to treat HAT [10,11]. Concerning the new chemical entities that are clinically studied by the Drug for Neglected Disease initiative (DNDi), only acoziborole (benzoxaborole derivative) is in phase IIb/III against HAT [10]. This quite limited drug portfolio calls for the research of new molecules that could strengthen the therapeutic arsenal and reduce the risk of emergence of resistant parasites.

Concerning fexinidazole, a 2-substituted-5-nitroimidazole derivative, it is a prodrug which is activated through the reduction of its nitro group by a NADH-specific type 1 nitroreductase (NTR), to generate electrophilic cytotoxic metabolites (nitroso and hydroxylamine derivatives) able to form covalent adducts with DNA and that are cytotoxic for the parasite [9,12]. Only one mitochondrial type 1 nitroreductase was identified in *Trypanosoma brucei* [13]. The particularity of nitroreductases is that they are absent in mammalian cells and then, constitute important targets for the development of new selective antiparasitic treatments. In this context, nitroaromatic compounds are key derivatives that have been and remain studied to fight against kinetoplastids, as shown with the structures of nifurtimox, fexinidazole and DNDI-0690, a novel 4-nitroimidazole derivative that is clinically studied against visceral leishmaniasis [14] (**Figure 1**).

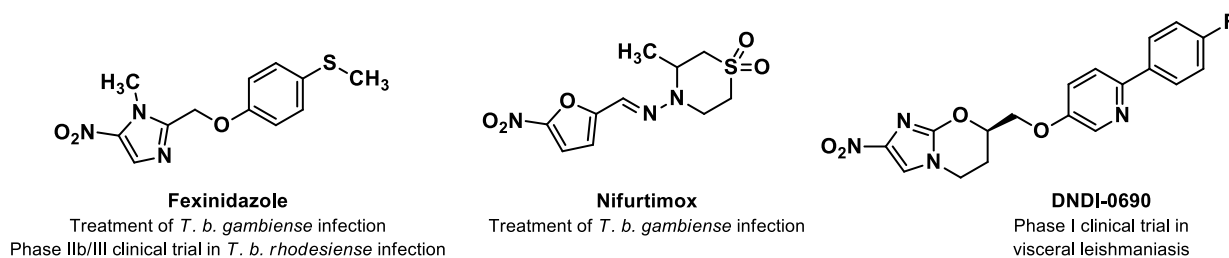
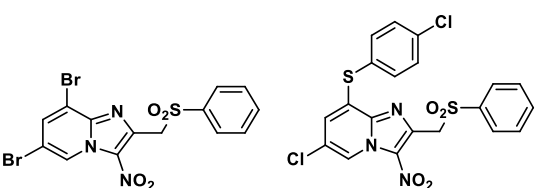


Figure 1. Structures of nitroheterocyclic drug-compounds that are marketed or clinically studied against *Trypanosoma brucei* and *Leishmania* infections.

Within the framework of our research program, focused on the development of original nitroheterocyclic antikinoplastid molecules, we formerly reported a first antileishmanial hit compound in 8-halogeno-3-nitroimidazo[1,2-*a*]pyridine series (hit A, **Figure 2**) [15]. Pharmacomodulation studies at position 8 of the scaffold were conducted and showed that introducing a 4-chlorophenylthio moiety improved *in vitro* antikinoplastid activity (hit B, **Figure 2**) [16]. However, hit-molecule A displayed limited water solubility while hit B showed a poor mouse liver microsomal stability ($T_{1/2} = 3$ min), even if some probable sulfoxide and sulfone metabolites remained active. Thus, to improve hydrosolubility, microsomal stability and antikinoplastid activity of this nitroheterocyclic series, we explored deeper the structure activity relationships by studying the influence of substituents at position 2 and 6 of the imidazo[1,2-*a*]pyridine ring and comparing to the activities of hits A and B.

Figure 2. Structures and biological profiles of previously identified antikinoplastid hit-compounds in 3-nitroimidazo[1,2-*a*]pyridine series [15–17].

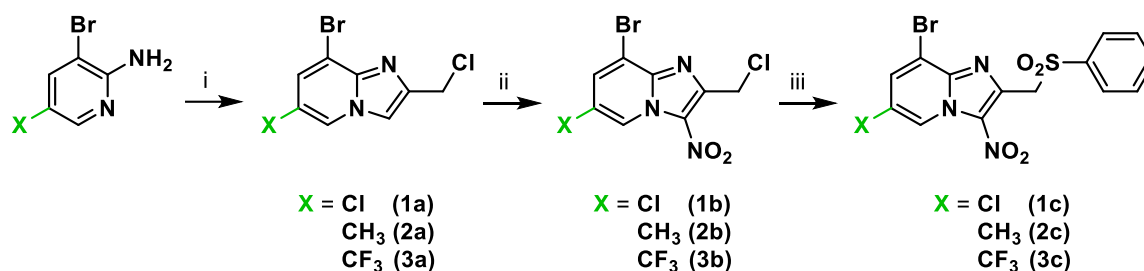


	Hit A	Hit B
EC ₅₀ <i>L. donovani</i> promastigotes (μM)	1.8	1.0
EC ₅₀ <i>L. donovani</i> amastigotes (μM)	5.5	1.3
EC ₅₀ <i>L. infantum</i> axenic amastigotes (μM)	4.4	1.7
EC ₅₀ <i>T. b. brucei</i> trypomastigotes (μM)	2.9	1.3
CC ₅₀ HepG2 (μM)	>31	>100

2. Results and discussion

To evaluate if redox potentials had an influence on the bioactivation of this chemical series by parasitic NTRs, analogs of hit A bearing a methyl group (electron donating) or a trifluoromethyl group (electron withdrawing) at position 6 of the imidazo[1,2-*a*]pyridine ring were synthesized. A bromine atom was not included in the pharmacomodulation study considering that we previously noted that molecules belonging to this series and bearing a bromine atom at position 6 showed the

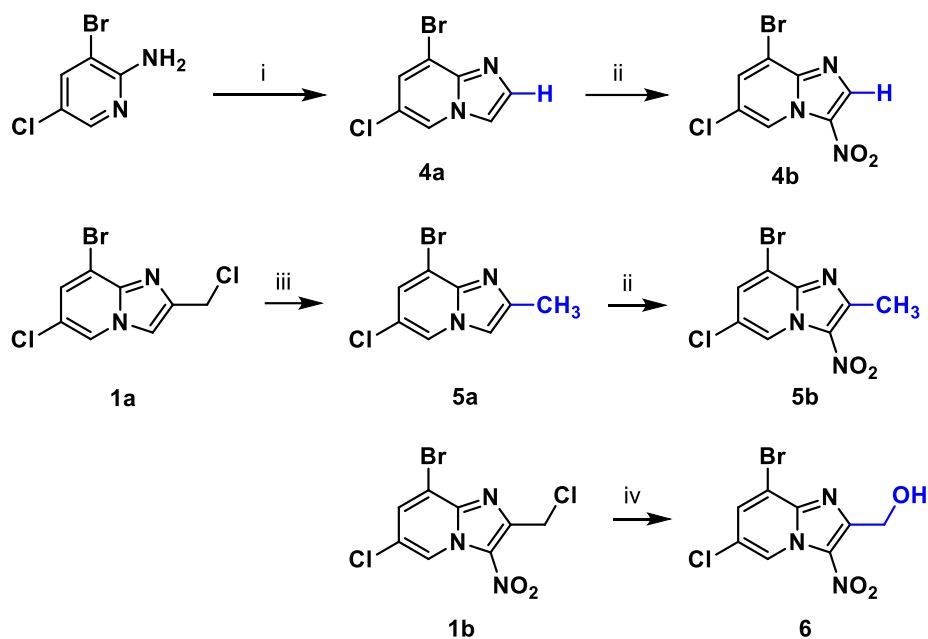
same level of antiparasitic activity as their chlorinated analogs, these latter presenting the advantage to show a better aqueous solubility. Thus, in parallel with the previously described 6-chloro analogue **1c** of hit A, new derivatives **2c** and **3c** were obtained through a 3-steps synthesis procedure (**Scheme 1**) that was previously reported [18,19].



Scheme 1. Synthesis of compounds **1a-c** to **3a-c**.

Reagents and conditions: (i) 1,3-Dichloroacetone 1.1 equiv, EtOH or DME, 80°C, 31% to 60%; (ii) HNO₃ 6 equiv, H₂SO₄, 0°C→RT, 51% to 85%; (iii) Sodium benzenesulfinate 3 equiv, DMSO, RT, 3 h, 57% to 89%.

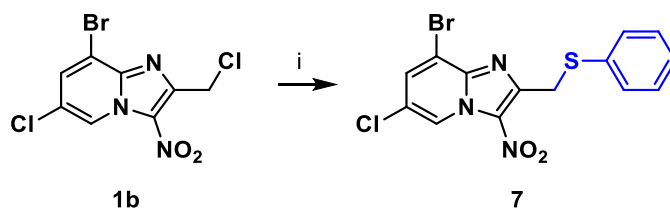
To study the influence of the substituent at position 2 of the imidazo[1,2-*a*]pyridine ring, the phenylsulfonylmethyl group encountered in the structures of hit A and B was modulated (**Scheme 2**). First, a 2-unsubstituted derivative (**4b**) was obtained through a cyclocondensation reaction of 2-amino-3-bromo-5-chloropyridine with chloroacetaldehyde, followed by a nitration reaction. Then, the 2-methyl-substituted derivative **5b** was synthesized by dehalogenation of **1a** followed by a nitration reaction of **5a** at position 3. Finally, the 2-hydroxymethyl-derivative **6** was obtained by hydrolysis of **1b** in the presence of copper sulfate in aqueous DMSO [20].



Scheme 2. Synthesis of compounds **4a-b**, **5a-b** and **6**.

Reagents and conditions: (i) Chloroacetaldehyde 1.5 equiv, NaHCO_3 2 equiv, EtOH, 80 °C, 31%; (ii) HNO_3 6 equiv, H_2SO_4 , 0°C→RT, 78% to 93%; (iii) NaBH_4 1 equiv, DMSO, RT, 63%; (iv) CuSO_4 1 equiv, DMSO/ H_2O (7.5:2.5), 100 °C, 32%.

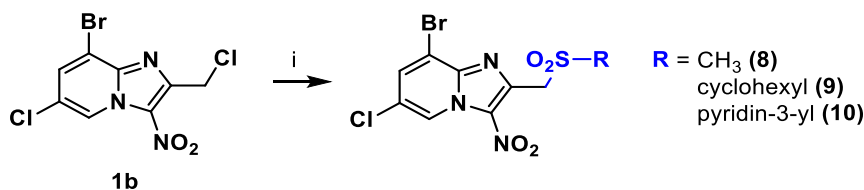
In order to explore the role of the sulfone moiety, an original 2-phenylthiomethyl derivative **7** was prepared from **1b** by a substitution reaction with sodium thiophenolate, formed *in situ* with NaH in DMSO at RT (**Scheme 3**), according to a protocol that we previously reported [21].



Scheme 3. Synthesis of compound **7**.

Reagents and conditions: (i) Thiophenol 1 equiv, NaH 1.1 equiv, DMSO, N_2 , RT, 28%.

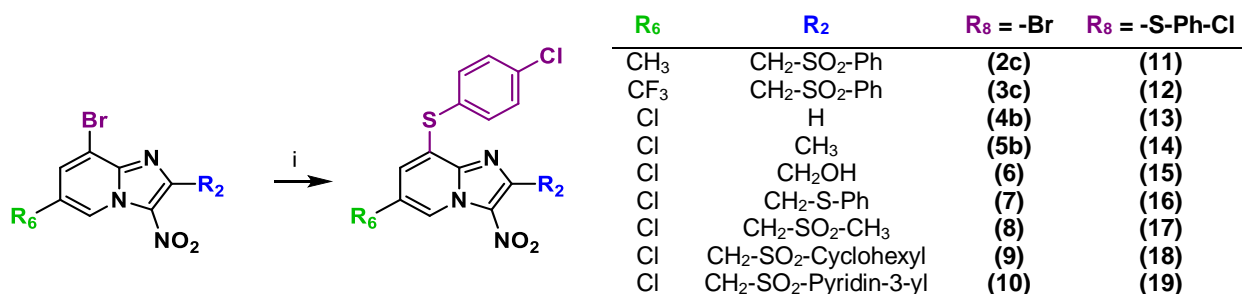
Then, the phenyl ring of the phenylsulfonylethyl moiety was replaced by a methyl, cyclohexyl or pyridin-3-yl group, using a previously described reaction [15] and leading to original derivatives **8-10** respectively, according to **Scheme 4**.



Scheme 4. Synthesis of compounds **8-10**.

Reagents and conditions: (i) Appropriate sulfonyl chloride 2 equiv, NaHCO₃ 2 equiv, Na₂SO₃ 2 equiv, EtOH/H₂O (1:1), N₂, 120 °C, MW, 22% to 47%.

To complete SAR data and allow comparison with hit B, nine derivatives (**11-19**) bearing a 4-chlorophenylthio moiety at position 8 were synthesized, applying a protocol that we previously reported in various nitroaromatic series with antiparasitic potential [22,23] (**Scheme 5**).

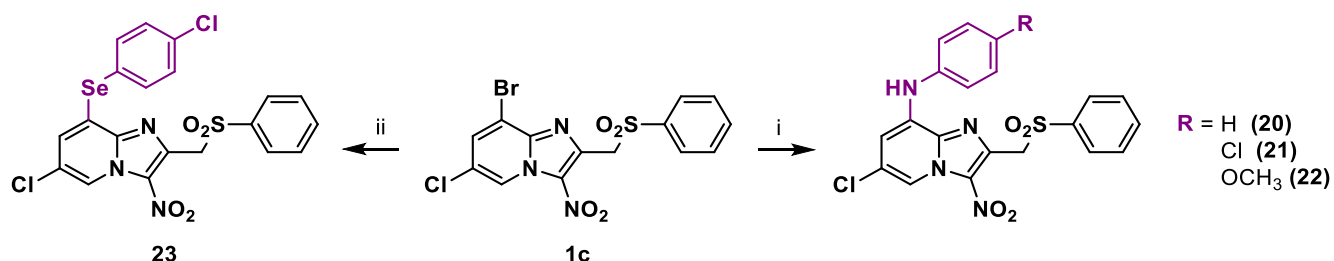


Scheme 5. Synthesis of compounds **11-19**.

Reagents and conditions: (i) 4-Chlorothiophenol 1 equiv, NaH 1 equiv, DMSO, N₂, RT, 20% to 90%.

Still by analogy with hit B, the influence of the heteroatom at position 8 was investigated deeper. First, the synthesis of 8-anilino derivatives *via* a Buchwald-Hartwig cross-coupling reaction was investigated (**Scheme 6**). The reaction conditions were studied by varying several parameters such as nature of base, nature and amount of catalyst and ligand, nature of solvent, and reaction

temperature. Three derivatives bearing an aniline moiety at position 8 were synthesized (**Scheme 6**) in moderate yields (42% to 52%). Then, a selenium analogue (**23**) of hit B was also prepared according to a previously described protocol [24], as presented in **Scheme 6**.

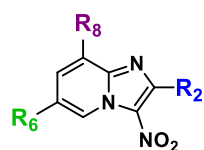


Scheme 6. Synthesis of 8-anilino derivatives **20-22** and 8-phenylselenanyl derivative **23**.

Reagents and conditions: (i) Appropriate aniline 1.2 equiv, Pd(OAc)₂ 0.08 equiv, *rac*-BINAP 0.15 equiv, K₂CO₃ 1.8 equiv, toluene, N₂, 140 °C, MW, 42% to 52 %; (ii) Bis(4-chlorophenyl)diselenide 0.5 equiv, NaBH₄ 2 equiv, PEG-400, N₂, 60 °C, 9 %.

Globally, ten molecules (analogues of hit A) bearing a bromine atom at position 8 of the imidazo[1,2-*a*]pyridine ring and 13 molecules (analogues of hit B) bearing a phenylthio, phenylamino or phenylselenanyl group at the same position were evaluated *in vitro*. Their influence on cell viability (cytotoxic concentration 50% = CC₅₀) was assessed on the HepG2 cell line, using doxorubicin as a positive control. *In vitro* antileishmanial activity (measured through effective concentration 50% = EC₅₀) was also measured on both the promastigote and axenic amastigote form of *L. donovani* and *L. infantum*, respectively. In parallel, the *in vitro* antitrypanosomal activity (EC₅₀) of these derivatives was determined on the trypomastigote blood stream form (BSF) of *T. b. brucei*. For all molecules, selectivity indices (SI) were calculated. Their antikinoplastid activity was compared to previous hit molecules and to commercially available reference drugs amphotericin B, miltefosine, fexinidazole, suramine, eflornithine and nifurtimox. The results are summarized in **Table 1**.

Table 1. *In vitro* evaluation of molecules **1c-23** on *L. donovani* promastigotes, *L. infantum* axenic amastigotes, *T. b. brucei* trypomastigotes (BSF) and on the human hepatocyte HepG2 cell line.



Compd	R ₂	R ₆	R ₈	Cell viability			Activity			
				CC ₅₀ HepG2 (μM)	EC ₅₀ <i>L. donovani</i> pro. (μM)	SI <i>L. donovani</i> pro.	EC ₅₀ <i>L. infantum</i> axenic ama. (μM)	SI <i>L. infantum</i> axenic ama.	EC ₅₀ <i>T. b. brucei</i> BSF (μM)	SI <i>T. b. brucei</i>
1c	-CH ₂ -SO ₂ -Ph	-Cl	-Br	>15.6 ^a	5.3 ± 0.3	>2.9	16.4 ± 0.2	>1	1.4 ± 0.4	>11.1
2c	-CH ₂ -SO ₂ -Ph	-CH ₃	-Br	>31.2 ^a	5.6 ± 1.4	>5.6	>3.1	-	1.2 ± 0.5	>26
3c	-CH ₂ -SO ₂ -Ph	-CF ₃	-Br	>15.6 ^a	6.2 ± 0.7	>2.5	>3.1	-	4.0 ± 2.7	>3.9
4b	-H	-Cl	-Br	16.2	9.3 ± 1.7	1.7	15.9 ± 0.7	1	0.4 ± 0.01	40.5
5b	-CH ₃	-Cl	-Br	>125 ^a	>12.5 ^c	-	32.1 ± 0.7	>3.9	>50 ^e	-
6	-CH ₂ -OH	-Cl	-Br	>125 ^a	>12.5 ^c	-	46.3 ± 1.4	>5.4	>50 ^e	-
7	-CH ₂ -S-Ph	-Cl	-Br	>31.2 ^a	>12.5 ^c	-	17.8 ± 0.8	>1.8	>50 ^e	-
8	-CH₂-SO₂-CH₃	-Cl	-Br	45	5.7 ± 1.4	7.9	>25^c	<1.8	0.017 ± 0.002	2647
9	-CH ₂ -SO ₂ -Cyclohexyl	-Cl	-Br	>15.6 ^a	0.9 ± 0.3	>17.3	>100 ^c	-	0.5 ± 0.07	>31.2
10	-CH ₂ -SO ₂ -Pyridin-3-yl	-Cl	-Br	>62.5 ^a	0.8 ± 0.3	>78	77.8 ± 0.8	>0.8	0.025 ± 0.005	2500
11	-CH ₂ -SO ₂ -Ph	-CH ₃	4-Cl-Ph-S-	>62.5 ^a	2.6 ± 0.4	>24	5.0 ± 0.3	12.5	1.8 ± 0.5	>34.7
12	-CH ₂ -SO ₂ -Ph	-CF ₃	4-Cl-Ph-S-	>7.8 ^a	1.9 ± 0.2	>4.1	-	-	0.17 ± 0.02	>45.9
13	-H	-Cl	4-Cl-Ph-S-	>7.8 ^a	2.5 ± 0.2	>3.1	-	-	0.085 ± 0.02	>92.8
14	-CH ₃	-Cl	4-Cl-Ph-S-	>7.8 ^a	>12.5 ^c	-	-	-	-	-
15	-CH ₂ -OH	-Cl	4-Cl-Ph-S-	>15.6 ^a	4.0 ± 0.3	>3.9	7.9 ± 0.3	>2	>50	-
16	-CH ₂ -S-Ph	-Cl	4-Cl-Ph-S-	>15.6 ^a	7.4 ± 0.4	>2.1	-	-	>50	-
17	-CH ₂ -SO ₂ -CH ₃	-Cl	4-Cl-Ph-S-	>31.2 ^a	1.2 ± 0.1	>26	10.3 ± 0.4	>3	0.067 ± 0.007	>465.7
18	-CH ₂ -SO ₂ -Cyclohexyl	-Cl	4-Cl-Ph-S-	>31.2 ^a	1.9 ± 0.1	>16.4	1.6 ± 0.2	>19.5	1.5 ± 0.1	>20.8
19	-CH ₂ -SO ₂ -Pyridin-3-yl	-Cl	4-Cl-Ph-S-	>31.2 ^a	0.5 ± 0.1	>62.4	0.8 ± 0.2	>39	1.2 ± 0.2	>26
20	-CH ₂ -SO ₂ -Ph	-Cl	Ph-NH-	>3.9 ^a	-	-	-	-	-	-
21	-CH ₂ -SO ₂ -Ph	-Cl	4-Cl-Ph-NH-	>3.9 ^a	-	-	-	-	-	-
22	-CH ₂ -SO ₂ -Ph	-Cl	4-CH ₃ O-Ph-NH-	>3.9 ^a	-	-	-	-	-	-
23	-CH ₂ -SO ₂ -Ph	-Cl	4-Cl-Ph-Se-	>7.8 ^a	0.7 ± 0.1	>11.1	0.9 ± 0.1	>8.7	0.3 ± 0.03	>26
Ref. 1	Hit A molecule			>31 ^a	1.8 ± 0.8	>17.2	4.4 ± 0.8	>7.1	2.9 ± 0.5	>10.7
Ref. 2	Hit B molecule			>100	1.0 ± 0.3	>100	1.7 ± 0.3	>58.8	1.3 ± 0.1	>76.9
Ref. 3	Doxorubicin ^b			0.2 ± 0.02	-	-	-	-	-	-
Ref. 4	Amphotericin B ^d			8.8 ± 0.3	0.07 ± 0.01	125.7	0.06 ± 0.001	146.7	-	-
Ref. 5	Miltefosine ^d			85 ± 8.8	3.1 ± 0.2	27.4	0.8 ± 0.2	106.3	-	-
Ref. 6	Fexinidazole ^{d,e}			>200 ^c	1.2 ± 0.2	>166.7	3.4 ± 0.8	>58.8	0.6 ± 0.2	>333
Ref. 7	Suramin ^e			>100 ^c	-	-	-	-	0.03 ± 0.009	>3333
Ref. 8	Eflornithine ^e			>100 ^c	-	-	-	-	13.3 ± 2.1	>7.5
Ref. 9	Nifurtimox ^e			45.2 ± 1.3	-	-	-	-	2.6 ± 0.8	17.4

^a The product could not be tested at higher concentrations due to a lack solubility in the culture medium

^b Doxorubicin was used as a cytotoxic reference drug

^c The EC₅₀ or CC₅₀ value was not reached at the highest tested concentration

^d Amphotericin B, Miltefosine and Fexinidazole were used as antileishmanial reference drugs

^e Fexinidazole, Suramin, Eflornithine and Nifurtimox were used as anti-*Trypanosoma brucei* reference drugs

^f SI = CC₅₀ HepG2 / EC₅₀ *L. infantum*

^g SI = CC₅₀ HepG2 / EC₅₀ *T. brucei brucei*

Bold: New antitrypanosomal hit

Out of the 23 tested molecules, 7 showed a poor aqueous solubility ($< 10 \mu\text{M}$) limiting their *in vitro* evaluation. Among them, 8-anilino-derivatives **20-22** were particularly insoluble in biological culture media, indicating that the aniline moiety should be avoided at position 8 of the antitrypanosomal scaffold. Regarding the effect on the cell viability of the HepG2 human cells, all molecules appeared as weakly cytotoxic ($15.6 \leq \text{CC}_{50} < 125 \mu\text{M}$) in comparison with doxorubicin ($\text{CC}_{50} = 0.2 \mu\text{M}$).

Then, 20 molecules were screened *in vitro* for their activity against *L. donovani* promastigotes and compared both to previous hit molecules and to amphotericin B, miltefosine and fexinidazole. Among them, only compounds **9**, **10**, **17**, **18** and **19**, bearing an alkyl- or pyridin-3-yl-sulfonylmethyl group at position 2, showed both good EC_{50} values ($0.5 \leq \text{EC}_{50} \leq 1.9 \mu\text{M}$) and good selectivity indices ($16 < \text{SI} < 78$). This suggests that a sulfonyl group in position 2 is needed to reach a good antileishmanial activity level on *L. donovani* promastigotes.

When considering the screening against *L. infantum* axenic amastigotes, out of the 5 molecules that were active on *L. donovani* promastigotes, only compounds **18** and **19** remained active ($0.8 \leq \text{EC}_{50} \leq 1.6 \mu\text{M}$) and selective ($19.5 < \text{SI} < 39$). These results confirmed that, in addition to a sulfonylmethyl substituent at position 2 of the imidazopyridine ring, antileishmanial activity was also favored when substituting position 8 by a thiophenol moiety. Unfortunately, compounds **18** and **19** were then evaluated on the intramacrophage amastigote stage of *L. donovani* and were not active ($\text{EC}_{50} > 10 \mu\text{M}$). Consequently, hit B still remains the most active antileishmanial molecule in this chemical series.

Regarding antitrypanosomal activity, molecules were tested on the blood stream form of *T. b. brucei* and compared to reference drugs fexinidazole, suramin, eflornithine and nifurtimox. Out of the 20 tested molecules, 8 displayed submicromolar activities ($0.017 \leq \text{EC}_{50} \leq 0.5 \mu\text{M}$), quite significantly better than the ones of hit A and B ($\text{EC}_{50} = 2.9$ and $1.3 \mu\text{M}$ respectively). Contrary to what was noted for antileishmanial activity, these 8 antitrypanosomal molecules are equally distributed between hit A (8-Br) and hit B (8-thiophenol) derivatives, showing that the

antitrypanosomal pharmacophore is less restrictive than the antileishmanial pharmacophore. Among these submicromolar active molecules, **8**, **9**, **10**, **12**, **17** and **23** presented a sulfonylmethyl moiety at position 2 whereas molecules **4b** and **13** were not substituted. Nevertheless, **4b** was the most cytotoxic derivative in the series and **13** showed a poor aqueous solubility. Then, as with antileishmanial activity, the sulfonylmethyl moiety seems to play a favorable role toward antitrypanosomal activity. When looking at hit A derivatives, methyl-, cyclohexyl- and pyridin-3-yl-sulfonylmethyl groups provided good to excellent activities (molecules **8-10**), showing that the substituent of the sulfonylmethyl moiety is a key modulation zone. Thus, molecule **8** appeared as the most active ($EC_{50} = 17$ nM) and selective ($SI = 2647$) antitrypanosomal molecule in the series. It was a lot more active than hits A and B ($EC_{50} = 2.9$ and 1.3 μ M respectively) but also more active than fexinidazole ($EC_{50} = 0.6$ μ M), suramin ($EC_{50} = 30$ nM), eflornithine ($EC_{50} = 13.3$ μ M) and nifurtimox ($EC_{50} = 2.6$ μ M). The selenium containing analog **23** of hit B appeared a lot less soluble in aqueous biological media than hit B despite being 4 times more active. Because of the same lack of water solubility, the 6-trifluoromethylated analogue **12** of hit B appeared less promising than other derivatives. Nevertheless, the comparison of the close activities of **11** and **12** toward hit B but also **2c** and **3c** toward **1c** and hit A, permitted to conclude that the antitrypanosomal pharmacophore allows small electron-donating or electron-withdrawing substituents such as CH_3 , Cl, Br or CF_3 at position 6.

From antitrypanosomal hit-molecule **8**, to deeper evaluate the influence of the sulfonylmethyl moiety, a 2-methylthiomethyl analog (**24**) was synthesized from substrate **1b**, using sodium methanethiolate as reagent (Table 2). Partial oxidation of the sulfur atom of **24** using *m*-CPBA in dichloromethane led to the sulfoxide derivative **25** (Table 2). The activities of **24** and **25** were evaluated *in vitro* for their activity against *T. b. brucei* and for their effect on cell viability on the HepG 2 cell line (Table 2). Thioether derivative **24** showed limited water solubility and modest antitrypanosomal activity ($EC_{50} = 2.2$ μ M) whereas sulfoxide derivative **25** was very active against *T. b. brucei* ($EC_{50} = 20$ nM) and displayed excellent selectivity index ($SI = 2570$). These results confirmed that position 2 was key to the antiparasitic activity and indicated that the

antitrypanosomal pharmacophore included either a sulfone or a sulfoxide functional group at position 2 of the imidazopyridine ring.

Table 2. Synthesis and biological activities of compounds **24** and **25**.

Compound	<i>T. brucei brucei</i> BSF EC ₅₀ (μM)	HepG2 CC ₅₀ (μM)	SI <i>T. b. brucei</i>
24	2.20 ± 0.24	>15.6 ^a	>7.1
25	0.020 ± 0.006	51.4 ± 8.3	2570

^aThe product could not be tested at higher concentrations due to a poor solubility in aqueous medium.
Reagents and conditions: (i) CH₃SNa 1 equiv, DMSO, RT, 52% (ii) *m*CPBA 1 equiv, CH₂Cl₂, 0 °C, 36%.

To assess the influence of the aforementioned modulations at position 2, 6 and 8 on the reduction potential of this nitroaromatic scaffold, an electrochemical study was conducted on several 3-nitroimidazo[1,2-*a*]pyridine derivatives using cyclic voltammetry. Experimental reduction potentials (**Figure 3**) were compared to the ones of fexinidazole, nifurtimox, and hit A (for 8-Br-derivatives) or hit B (for 8-phenylthio-derivatives). For all tested compounds, a reversible single electron reduction was observed and attested the formation of a nitro radical anion. The redox potentials were measured and the values were corrected versus Normal Hydrogen Electrode (NHE). These values ranged from -0.58 V to -0.79 V, in comparison with the ones of nifurtimox ($E^0 = -0.61$ V) and fexinidazole ($E^0 = -0.83$ V). There was almost no difference in redox potential values when comparing hit A with hit B analogues, bearing the same substituents at positions 2 and 6: the electronic effect of the bromine atom or of the *p*-chlorothiophenol group at position 8 were almost the same. Introducing an aniline moiety at position 8 of the imidazopyridine ring

(molecule **20**, $E^0 = -0.69$ V) had the same effect toward the redox potential value as a phenyl moiety [17] but allowed to reach a lower E^0 value than with a *p*-chlorothiophenol moiety (hit **B**, $E^0 = -0.63$ V). Modifying the substituent at position 6 of the imidazopyridine ring had a strong influence toward the reducibility of the nitro group: 6-trifluoromethyl-derivatives (**3c** and **12**) displayed high E^0 values (-0.60 to -0.58 V) whereas 6-methyl-derivatives (**2c** and **11**) presented the lowest E^0 values (-0.76 V) among the derivatives presenting a phenylsulfonylmethyl side chain at position 2. There was also an important influence of the substituent at position 2 toward E^0 values. Switching from phenylsulfonylmethyl derivatives **1c** or **hit B** (E^0 values = -0.65 V and -0.63 V) to their phenylthiomethyl analogues **7** or **16** provided molecules with lower E^0 values (-0.70 and -0.72 V respectively). This effect that was rather comparable to the one noted with the hydrogen atom when comparing **16** to **13** ($E^0 = -0.74$ V). This decrease in E^0 value was even more acute when introducing a methyl group at position 2 (molecule **14**, $E^0 = -0.79$ V). Finally, by comparing the E^0 values of compounds **1c** and **8**, it appeared that replacing the phenylsulfonylmethyl group by a methylsulfonylmethyl one was responsible for a significant increase in the redox potential values from -0.65 to -0.60 V. Nevertheless, no correlation between redox potential values and antiparasitic EC_{50} values could be noted in the studied series.

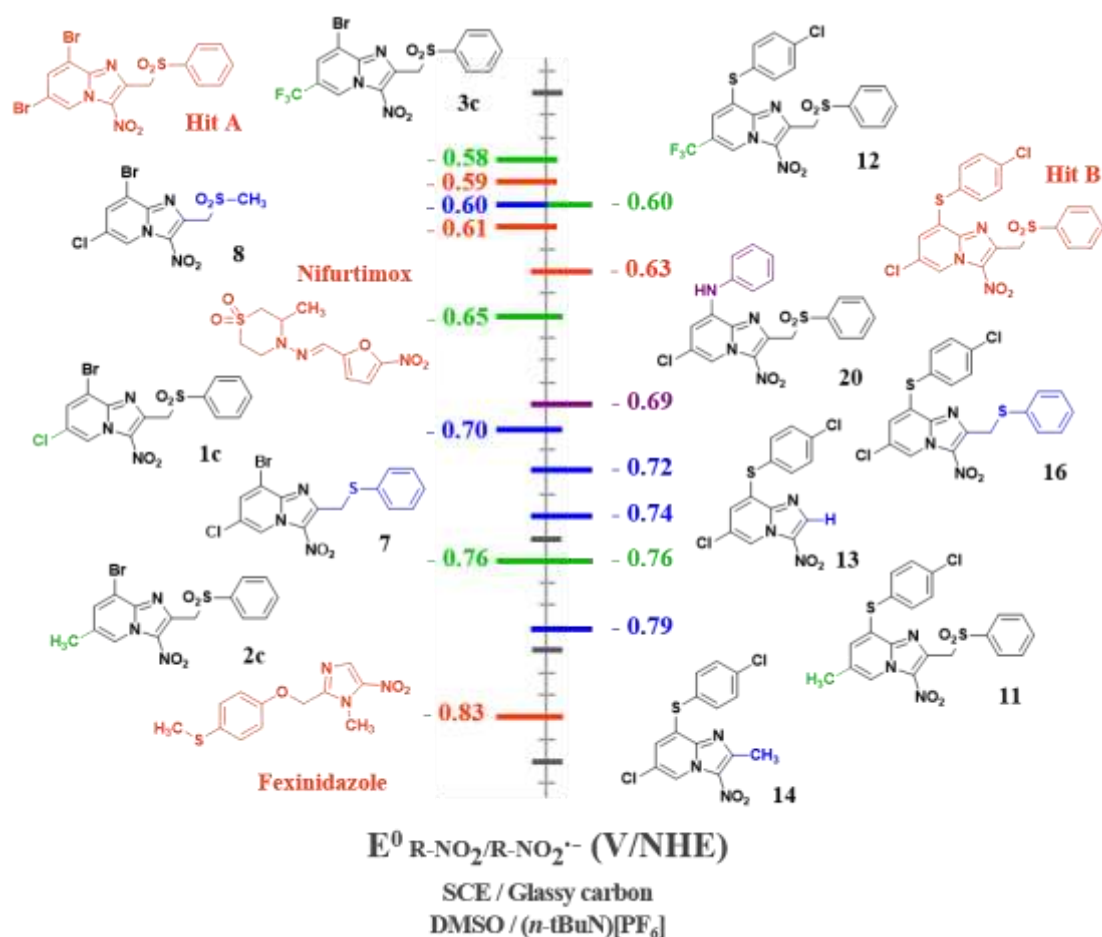


Figure 3. Redox potentials (E^0) of Hit **A** (left) and Hit **B** (right) derivatives determined by cyclic voltammetry and given versus NHE. Conditions: selected compounds (10^{-3} mol.L $^{-1}$) in non-aqueous medium (DMSO + 0.1 mol.L $^{-1}$ (*n*-Bu $_4$ N)[PF $_6$]) on GC microdisk ($r = 0.5$ mm) at room temperature. Scan rate: 0.2 V.s $^{-1}$.

These molecules being probable substrates of parasitic nitroreductases, the mechanism of bioactivation of molecule **8** in the *Trypanosoma* cell was investigated by comparing the EC $_{50}$ values measured on a wild-type strain with the one measured on a NTR-overexpressing strain. This assay confirmed that, like for nifurtimox and for all previous hit molecules studied in 3-nitroimidazopyridine series, molecule **8** was bioactivated by *T. b. brucei* type 1 NTR as the EC $_{50}$ value of **8** on the NTR-overexpressing strain was 4 times lower than on the wild-type strain. (**Figure 4**). Noticeably, compound **8** was almost thirty times more active on *T. b. brucei* wild-type strain than nifurtimox.

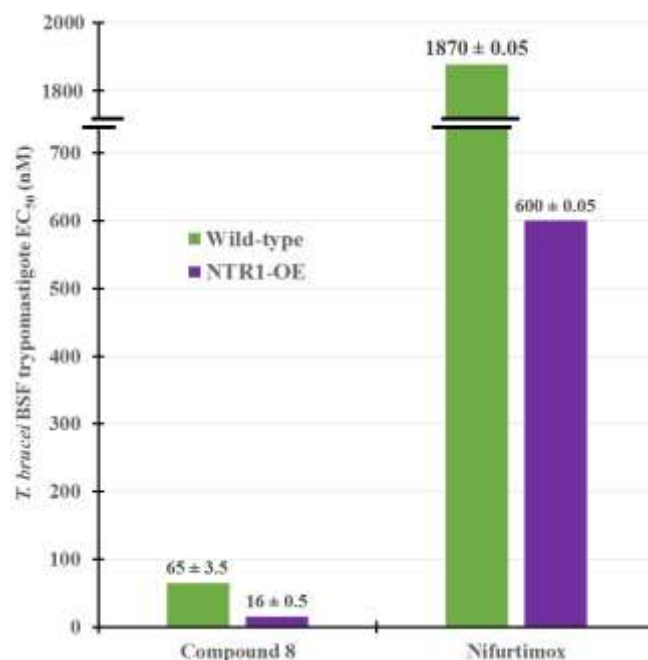


Figure 4. Sensitivity of wild-type and NTR-overexpressing *T. brucei* BSF trypomastigotes strains toward hit molecule **8** and nifurtimox control.

The 3-amino-analogue **26** of hit compound **8** was also synthesized and evaluated *in vitro* to confirm the essentiality of the nitro group for antikinoplastid activity. Molecule **26** was prepared by reduction of **8** in the presence of iron powder in refluxing acetic acid (**Table 3**). As expected, **26** did not show any antileishmanial activity and displayed a poor antitrypanosomal activity ($EC_{50} = 7.2 \mu\text{M}$). These results are consistent with the hypothesis that these 3-nitroimidazo[1,2-*a*]pyridines require bioactivation by parasitic NTRs, making the nitro group an essential element of the antikinoplastid pharmacophore.

Table 3. Synthesis and biological activities of compounds **26**.

8 **26**

Compound	<i>L. donovani</i> promastigotes EC ₅₀ (μM)	<i>L. infantum</i> axenic amastigotes EC ₅₀ (μM)	<i>T. brucei brucei</i> BSF EC ₅₀ (μM)	HepG2 CC ₅₀ (μM)
26	>12.5 ^a	>100 ^a	7.2 ± 0.8	>125 ^b

^a The EC₅₀ or CC₅₀ value was not reached at the highest tested concentration.

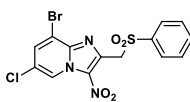
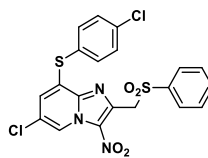
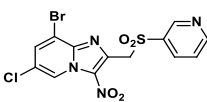
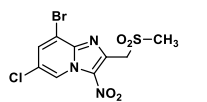
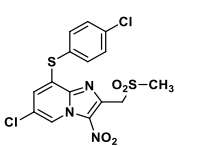
^b The product could not be tested at higher concentrations due to a poor solubility in aqueous medium.

Reagents and conditions: (i) Fe⁰ powder 10 equiv, AcOH, reflux, 30 min, 40 %.

The poor microsomal stability of hit molecules A and B was a limiting PK parameter for further development of the series (hit A $T_{1/2} = 9$ min and hit B $T_{1/2} = 3$ min; $T_{1/2}$ of propranolol control = 26 min), although some metabolites of hit B remained active *in vitro* against *Leishmania* spp [16]. For that reason, more polar, ionizable or less lipophilic pyridin-3-yl- or methyl-sulfonylmethyl-derivatives **8**, **10** and **17** of hit B and **1c** were evaluated *in vitro* for their microsomal stability (**Table 4**). As expected, microsomal stability was greatly improved when changing the phenyl ring (**1c**, $T_{1/2} = 12$ min) with a pyridine one (**10**, $T_{1/2} = 27$ min) and even better with a methyl group (**8**, $T_{1/2} > 40$ min). Effectively, molecules **10** and **8** were less lipophilic and more water-soluble than compound **1c**, but some microsomal *N*-oxidation can possibly be anticipated on the pyridine moiety of **10**. Even if real, this improvement in microsomal stability was less concluding comparing hit B to **17**, most probably because the sulfur atom of the thiophenol moiety remains actively oxidized by microsomes in **17**. Thus, positions 2 and 6 of the imidazopyridine ring appeared as essential modulation sites for increasing microsomal stability. Besides, the binding of molecule **8** to human albumin was logically much lower than all other derivatives as the two aromatic rings that substitute the imidazopyridine ring in hit B (thiophenol and phenylsulfonylmethyl moieties) were avoided, leading to a decarbonated scaffold with lower

molecular weight. Reducing the binding to human albumin could be an important parameter to control so as to optimize future *in vivo* activity that can be restricted by insufficient distribution.

Table 4. *In vitro* pharmacokinetic data of selected key compounds.

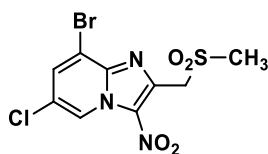
					
	1c	Hit B	10	8	17
Binding to human albumin (%)	96.5	99.9	87.0	76.9	98.9
Microsomal stability: T _{1/2} (min)	12	3	27	>40	12

Some important physicochemical parameters of hit molecule **8** were also calculated or measured (**Table 5**): molecule **8** showed average lipophilicity (cLogP = 1.14) and was 20 times more soluble in water than hit B (thermodynamic solubility of **8** = 26 μ M versus 1.4 μ M for hit B) [16].

The mutagenicity of many nitroheterocyclic molecules towards bacteria or parasites has been known for many years [25], the reduction of the nitro group being at the origin of this property. For fexinidazole, nitroreductase-dependent mutagenic activity was observed in the Ames test. However, its genotoxicity evaluation in the micronucleus assay was negative for the native molecule and its two metabolites [26]. This result suggests that the Ames test, the international reference test for measuring the mutagenicity of a molecule *in vitro* [27], is not suitable for the evaluation of nitroheterocyclic molecules. Indeed, since they undergo metabolic activation by *Salmonella* type 1 NTRs during the test, it appears difficult to extrapolate their genotoxicity profile to humans. Thus, to overcome the presence of bacterial nitroreductases expressed by the *Salmonella* strains used in the Ames test, a study of the genotoxicity of compound **8** was carried out using two complementary assays. First, a micronucleus test was conducted on the CHO-K1

cell line, both with and without addition of the metabolizing S9 mixture (see supplementary material). Molecule **8** showed no significant increase in micronucleated cell rates for all the tested concentrations (0.01 mM to 0.5 mM), either in the absence or presence of S9 mix, indicating that molecule **8** does not exert cytogenetic effects in CHO cells in culture and does not produce metabolites with cytogenetic effects. Then a comet assay was carried out on the HepG2 cell line at 5, 10 and 20 μ M, exposing cells with compound **8** for 2, 24 or 72 h and using methyl methanesulfonate as a positive control (supplementary material): the values of % DNA in tail were similar to the ones obtained in control cells. The negative results of these 2 assays are consistent with those obtained with previously studied hit molecules in the series and also with those of fexinidazole that is also devoid of mutagenic properties.

Finally, an *in vivo* toxicity study of molecule **8** was carried out to determine its maximal tolerated dose. A group of 4 mice received a once daily repeated oral (intra-gastrical gavage) dose of molecule **8** at 100 mg/kg for 5 days, and a follow-up was performed. As no side effect was detected, the No Observed Adverse Event Level (NOAEL) in mice was set at 100 mg/kg/day. A post-mortem examination revealed no lesion on different organs (brain, lung, heart, liver and kidney). Thereafter, a pharmacokinetic analysis was performed to identify the behavior of molecule **8** after oral administration. The main pharmacokinetic parameters are presented in **Table 5**. Compound **8** was orally absorbed and showed good systemic exposure. It displayed a long half-time (7.7 h) and, with a T_{max} of 5 h, a single daily administration could be considered for further experiments. A PAMPA BBB assay finally showed the possibility for molecule **8** to cross the blood-brain barrier by a moderate passive diffusional way, in accordance with its CNS MPO score (5.8) [28].

Table 5. Physicochemical, pharmacokinetic and genotoxic data regarding hit compound **8**.

cLogP ^a	1.14
Thermodynamic solubility (μM)	25.8 ± 0.6
PAMPA blood-brain barrier permeability assay : P _e (nm/s)	84.2 ± 2.9
CNS MPO score	5.8
C _{max} in mouse (ng/mL)	741 ± 580
T _{max} in mouse (h)	5.0 ± 5.2
Plasma half-life in mouse (h)	7.7 ± 1.3
AUC _{0-inf} (ng.h/mL)	7060 ± 693
Clearance (mL/h)	0.51 ± 0.05
Micronucleus assay (@ 10, 50, 100 and 500 μM +/- S9mix)	Negative
Comet assay (@ 5, 10 and 20 μM for 2, 24 and 72 h)	Negative

^a Weighted clogP was computed by Marvin[®] (ChemAxon)

3. Conclusion

This antikinoplastid SAR study was conducted through the synthesis and evaluation of 26 original imidazo[1,2-*a*]pyridine derivatives. Although most of these molecules displayed modest to good *in vitro* antileishmanial activity on the promastigote form of *L. donovani*, they were ineffective on the axenic amastigote form of *L. infantum* and/or the intramacrophage amastigote form of *L. donovani*. However, nine of these compounds showed submicromolar EC₅₀ values on *T. b. brucei* bloodstream form and low cytotoxicities on the HepG2 cell line, including 3 molecules with a selectivity index ≥2500. In this series, positions 2 and 6 appeared as key positions for modulating the reduction potential of these nitroheterocycles while maintaining their antitrypanosomal activity. Position 2 also allowed to improve mouse liver microsomal stability, as illustrated by the best molecule in this series (**8**) bearing a methylsulfonylmethyl group instead of the phenylsulfonylmethyl group found in previous hit molecules A and B. Indeed, in addition to its very good *in vitro* activity on *T. b. brucei* BSF (better than the ones of all reference compounds), its *in vitro* microsomal stability was >40 min and therefore greatly increased in comparison with

previous imidazopyridine hit molecules that we reported. Compound **8** also displayed increased water solubility, appeared BBB-permeable in a PAMPA assay and was shown to be bioactivated by type 1 parasitic NTR. Moreover, this derivative was not genotoxic, neither the micronucleus assay nor in the comet assay, which could represent a significant improvement over nitroaromatic antitypanosomal drugs like nifurtimox. In the mouse, molecule **8** was orally absorbed and well tolerated after repeated administrations of 100 mg/kg for 5 days. Its long plasma half-life (7.7 h) is encouraging and opens the way for a hit to lead program searching for novel antikinoplastid drug candidates.

4. Experimental section

4.1. Organic synthesis and characterizations

Commercial reagents were used as received without additional purification. Melting points were determined in open capillary tubes with a Büchi apparatus and are uncorrected. Elemental analysis and HRMS were carried out at the Spectropole, Faculté des Sciences et Techniques de Saint-Jérôme, Marseille, France. NMR spectra were recorded on a Bruker ARX 200 spectrometer or a Bruker AV 250 spectrometer at the Faculté de Pharmacie de Marseille, or a BRUKER Avance III nanobay 400 spectrometer at the the Spectropole, Faculté des Sciences et Techniques de Saint-Jérôme, Marseille, or on a Bruker UltraShield 300 MHz or a Bruker IconNMR 400 MHz spectrometer at the Laboratoire de Chimie de Coordination, Toulouse ($^1\text{H-NMR}$: 200, 250, 300 or 400 MHz, $^{13}\text{C-NMR}$: 50, 63, 75 or 100 MHz). NMR references were the following: ^1H : CHCl_3 $\delta = 7.26$, $\text{DMSO-}d_6$ $\delta = 2.50$ and ^{13}C : CHCl_3 $\delta = 76.9$, $\text{DMSO-}d_6$ $\delta = 39.5$. Solvents were dried by conventional methods. The following adsorbent was used for column chromatography: silica gel 60 (Merck, particle size 0.063–0.200 mm, 70–230 mesh ASTM). TLC was performed on 5 cm \times 10 cm aluminum plates coated with silica gel 60F-254 (Merck) in an appropriate eluent. Visualization was made with ultraviolet light (254 nm). HRMS spectra were recorded on QStar

Elite (Applied Biosystems SCIEX) spectrometer. PEG was the matrix for HRMS. The experimental exact mass was given for the ion which has the maximum isotopic abundance. Purity of synthesized compounds was checked with LC-MS analyses which were realized at the Faculté de Pharmacie de Marseille with a Thermo Scientific Accela High Speed LC System[®] coupled with a single quadrupole mass spectrometer Thermo MSQ Plus[®]. The RP-HPLC column used is a Thermo Hypersil Gold[®] 50 × 2.1 mm (C18 bounded), with particles of 1.9 μm diameter. The volume of sample injected on the column was 1 μL. The chromatographic analysis, total duration of 8 min, is made with the gradient of following solvents: t = 0 min, water/methanol 50/50; 0 < t < 4 min, linear increase in the proportion of methanol to a ratio water/methanol 5/95; 4 < t < 6 min, water/methanol 5/95; 6 < t < 7 min, linear decrease in the proportion of methanol to return to a ratio 50/50 water/methanol; 6 < t < 7 min, water/methanol 50/50. The water used was buffered with 5 mM ammonium acetate. The retention times (t_R) of the molecules analyzed are indicated in min.

Compounds **1a**, **1b** and **1c** were prepared as previously described [17].

4.1.1. 8-Bromo-2-chloromethyl-6-methylimidazo[1,2-a]pyridine (**2a**)

To a solution of 3-bromo-5-methylpyridin-2-amine (2 g, 10.1 mmol, 1 equiv.) in ethanol (100 mL), 1,3-dichloroacetone (1.46 g, 11.8 mmol, 1.1 equiv.) was added. The reaction mixture was stirred and heated under reflux for 72 h. The solvent was then evaporated *in vacuo*. Compound **2a** was obtained, after purification by chromatography on silica gel (eluent: cyclohexane–ethyl acetate 6.5:3.5) and recrystallization from propan-2-ol as a beige solid in 31% yield (0.82 g). mp: 151 °C. ¹H NMR (300 MHz, CDCl₃) δ: 2.31 (3H, s), 4.79 (2H, s), 7.33 (1H, d, *J* = 1.4 Hz), 7.63 (1H, s), 7.84 (1H, t, *J* = 1.2 Hz). ¹³C NMR (100 MHz, CDCl₃) δ: 18.0 (CH₃), 39.7 (CH₂), 111.0 (C), 112.53 (CH), 122.9 (C), 123.0 (CH), 130.7 (CH), 142.4 (C), 143.9 (C). LC/MS ESI⁺ t_R 1.77 min, (m/z) [M+H]⁺ 259.08/261.09/263.12. HRMS (+ESI): 260.9609 (M + H⁺). Calcd for C₉H₈BrClN₂: 260.9610.

4.1.2. 8-Bromo-2-chloromethyl-6-methyl-3-nitroimidazo[1,2-*a*]pyridine (**2b**)

To a solution of 8-bromo-2-chloromethyl-6-methylimidazo[1,2-*a*]pyridine **2a** (0.8 g, 3.09 mmol, 1 equiv.) in concentrated sulfuric acid (8 mL) cooled by an ice-water bath, nitric acid 65% (850 μ L, 18.5 mmol, 6 equiv.) was added. The reaction mixture was stirred for 1 h at room temperature. Then, the mixture was slowly poured into an ice-water mixture and the desired product precipitated. The beige solid was collected by filtration, dried under reduced pressure and recrystallized from propan-2-ol to give the expected product **2b** in 85% yield (0.8 g). mp 179 °C. ^1H NMR (400 MHz, CDCl_3) δ : 2.51 (3H, d, $J = 0.8$ Hz), 5.10 (2H, s), 7.79 (1H, d, $J = 1.1$ Hz), 9.24–9.25 (1H, m). ^{13}C NMR (100 MHz, $\text{DMSO-}d_6$) δ : 17.6 (CH_3), 31.1 (CH_2), 110.8 (C), 125.4 (CH), 126.1 (C), 128.0 (C), 136.5 (CH), 140.8 (C), 146.5 (C). LC/MS ESI⁺ t_{R} 2.04 min, (m/z) $[\text{M}+\text{H}]^+$ 304.44/305.80/307.06. HRMS (+ESI): 305.9461 (M + H⁺). Calcd for $\text{C}_9\text{H}_7\text{BrClN}_3\text{O}_2$: 305.9461.

4.1.3. 8-Bromo-6-methyl-3-nitro-2-(phenylsulfonylmethyl)imidazo[1,2-*a*]pyridine (**2c**)

To a solution of 8-bromo-2-chloromethyl-6-methyl-3-nitroimidazo[1,2-*a*]pyridine **2b** (0.5 g, 1.64 mmol, 1 equiv.) in dimethylsulfoxide (30 mL), sodium benzenesulfinate (0.81 g, 4.93 mmol, 3 equiv.) was added. The reaction mixture was stirred for 3 h at room temperature. The reaction mixture was then slowly poured into an ice-water mixture, making the desired product precipitate. The pale yellow solid was collected by filtration, dried under reduced pressure and recrystallized from acetonitrile to give the expected product **2c** in 89% yield (0.6 g). mp 202 °C. ^1H NMR (200 MHz, CDCl_3) δ : 2.50 (3H, d, $J = 0.8$ Hz), 5.17 (2H, s), 7.52–7.57 (2H; m), 7.67 (1H, tt, $J = 1.3$ and 7.4 Hz), 7.76 (1H, d, $J = 1.5$ Hz), 7.86–7.89 (2H, m), 9.19–9.20 (1H, m). ^{13}C NMR (50 MHz, CDCl_3) δ : 18.6 (CH_3), 57.0 (CH_2), 112.4 (C), 124.9 (CH), 128.0 (C), 128.7 (2CH), 129.3 (2CH), 131.7 (C), 134.3 (CH), 136.1 (CH), 139.3 (C), 139.4 (C), 141.7 (C). LC/MS ESI⁺ t_{R} 1.81 min, (m/z) $[\text{M}+\text{H}]^+$ 409.90/411.89/412.98. HRMS (+ESI): 411.9750 (M + H⁺). Calcd for $\text{C}_{15}\text{H}_{12}\text{BrN}_3\text{O}_4\text{S}$: 411.9785.

4.1.4. 8-Bromo-2-chloromethyl-6-(trifluoromethyl)imidazo[1,2-*a*]pyridine (**3a**)

To a solution of 3-bromo-5-trifluoromethylpyridin-2-amine (1 g, 4.15 mmol, 1 equiv.) in 1,2-dimethoxyethane (60 mL), 1,3-dichloroacetone (0.58 g, 4.56 mmol, 1.1 equiv.) was added. The reaction mixture was stirred and heated under reflux for 72 h. The solvent was then evaporated *in vacuo* and the product **3a** was directly involved in the next synthesis step, without being isolated. ¹H NMR (200 MHz, CDCl₃) δ: 5.55 (2H, s), 7.62–7.71 (1H, m), 7.84–7.95 (1H, m), 8.22–8.32 (1H, m). LC/MS ESI⁺ t_R 2.49 min, (m/z) [M+H]⁺ 312.9/314.99/316.93.

4.1.5. 8-Bromo-2-chloromethyl-3-nitro-6-(trifluoromethyl)imidazo[1,2-*a*]pyridine (**3b**)

To a solution of 8-bromo-2-chloromethyl-6-(trifluoromethyl)imidazo[1,2-*a*]pyridine **3a** (1 g, 3.19 mmol, 1 equiv.) in concentrated sulfuric acid (12 mL) cooled by an ice-water bath, nitric acid 65% (1 mL, 19.14 mmol, 6 equiv.) was added. The reaction mixture was stirred for 1 h at room temperature. Then, the mixture was slowly poured into an ice-water mixture with sodium carbonate and extracted three times with dichloromethane. The organic layer was washed three times with brine, dried over MgSO₄, filtered and evaporated. The crude residue was purified by column chromatography on silica gel (eluent: dichloromethane) and compound **3b** was isolated as a white solid in 51% yield (0.58 g). mp 143 °C. ¹H NMR (200 MHz, CDCl₃) δ: 5.11 (2H, s), 8.06 (1H, d, *J* = 1.5 Hz), 9.75–9.77 (1H, m). ¹³C NMR (50 MHz, CDCl₃) δ: 38.1 (CH₂), 114.3 (C), 121.6 (C, q, *J* = 35.5 Hz), 122.1 (C, q, *J* = 272.9 Hz), 125.6 (CH, q, *J* = 5.5 Hz), 129.1 (CH, d, *J* = 2.6 Hz), 130.5 (C), 142.5 (C), 148.8 (C). LC/MS ESI⁺ t_R 2.83 min, (m/z) [M+H]⁺ 357.97/358.95. HRMS (+ESI): 357.9202 (M + H⁺). Calcd for C₉H₄BrClF₃N₃O₂: 357.9200.

4.1.6. 8-Bromo-3-nitro-2-(phenylsulfonylmethyl)-6-(trifluoromethyl)imidazo[1,2-*a*]pyridine (**3c**)

To a solution of 8-bromo-2-chloromethyl-3-nitro-6-(trifluoromethyl)imidazo[1,2-*a*]pyridine **3b** (0.5 g, 1.4 mmol, 1 equiv.) in dimethylsulfoxide (40 mL), sodium benzenesulfinate (0.69 g, 4.18

mmol, 3 equiv.) was added. The reaction mixture was stirred for 2 h at room temperature. Then, the mixture was slowly poured into an ice-water mixture and extracted three times with dichloromethane. The organic layer was washed five times with brine, dried over MgSO₄, filtered and evaporated. The crude residue was recrystallized from acetonitrile to obtain the expected product **3c** as a white solid in 57% yield (0.37 g). mp 210 °C. ¹H NMR (200 MHz, CDCl₃) δ: 5.20 (2H, s), 7.55–7.62 (2H, m), 7.68–7.72 (1H, m), 7.88–7.93 (2H, m), 8.05–8.06 (1H, m), 9.74–9.75 (1H, m). ¹³C NMR (50 MHz, CDCl₃) δ: 56.6 (CH₂), 114.1 (C), 121.5 (C, q, *J* = 35.5 Hz), 122.1 (C, q, *J* = 273.4 Hz), 125.3 (CH, q, *J* = 5.4 Hz), 128.5 (2CH), 129.1 (CH, d, *J* = 2.5 Hz), 129.3 (2CH), 132.5 (C), 134.4 (CH), 139.0 (C), 140.6 (C), 142.4 (C). LC/MS ESI⁺ t_R 2.76 min, (m/z) [M+H]⁺ 463.74/465.78/468.23. HRMS (+ESI): 465.9499 (M + H⁺). Calcd for C₁₅H₉BrF₃N₃O₄S: 465.9502.

4.1.7. 8-Bromo-6-chloroimidazo[1,2-*a*]pyridine (**4a**)

To a solution of 3-bromo-5-chloropyridin-2-amine (10 g, 48.2 mmol, 1 equiv.) in ethanol (150 mL), chloroacetaldehyde (6.69 g, 72.3 mmol, 1.5 equiv.) and sodium bicarbonate (6.86 g, 81.6 mmol, 2 equiv.) were added. The reaction mixture was stirred and heated under reflux for 96 h. Then, the mixture was slowly poured into an ice-water mixture and extracted three times with dichloromethane. The organic layer was washed three times with brine, dried over MgSO₄, filtered and evaporated. Compound **4a** was obtained, after purification by chromatography on silica gel (eluent: dichloromethane) and recrystallization from propan-2-ol as a pale beige solid in 31% yield (3.48 g). mp: 131 °C. ¹H NMR (300 MHz, DMSO-*d*₆) δ: 7.68 (1H, d, *J* = 1.2 Hz), 7.74 (1H, d, *J* = 1.8 Hz), 8.05 (1H, d, *J* = 1.2 Hz), 8.90 (1H, d, *J* = 1.8 Hz). ¹³C NMR (75 MHz, DMSO-*d*₆) δ: 110.9 (C), 111.8 (C), 116.0 (CH), 118.3 (C), 124.8 (CH), 127.3 (CH), 134.4 (CH). LC/MS ESI⁺ t_R 1.21 min, (m/z) [M+H]⁺ 231.09/233.09/235.10. HRMS (+ESI): 232.9300 (M + H⁺). Calcd for C₇H₄BrClN₂: 232.9297.

4.1.8. 8-Bromo-6-chloro-3-nitroimidazo[1,2-*a*]pyridine (**4b**)

To a solution of 8-bromo-6-chloroimidazo[1,2-*a*]pyridine **4a** (0.5 g, 2.16 mmol, 1 equiv.) in concentrated sulfuric acid (5 mL) cooled by an ice-water bath, nitric acid 65% (500 μ L, 13 mmol, 6 equiv.) was added. The reaction mixture was stirred for 1 h at room temperature. Then, the mixture was slowly poured into an ice-water mixture with potassium carbonate and extracted three times with dichloromethane. The organic layer was washed three times with brine, dried over MgSO₄, filtered and evaporated. Compound **4b** was obtained, after purification by chromatography on silica gel (eluent: dichloromethane) and recrystallization from propan-2-ol as a beige solid in 93% yield (0.56 g). mp 145 °C. ¹H NMR (400 MHz, CDCl₃) δ : 7.90 (1H, d, *J* = 1.8 Hz), 8.65 (1H, s), 9.46 (1H, d, *J* = 1.8 Hz). ¹³C NMR (100 MHz, CDCl₃) δ : 113.4 (C), 124.3 (CH), 125.0 (C), 130.2 (C), 133.4 (CH), 138.1 (CH), 148.0 (C). LC/MS ESI⁺ *t*_R 1.42 min, (m/z) [M+H]⁺ 275.98/276.96/277.58. HRMS (+ESI): 277.9149 (M + H⁺). Calcd for C₇H₃BrClN₃O₂: 277.9148.

4.1.9. 8-Bromo-6-chloro-2-methylimidazo[1,2-*a*]pyridine (**5a**)

To a solution of sodium borohydride (0.07 g, 1.79 mmol, 1 equiv.) in dimethylsulfoxide (60 mL), 8-bromo-6-chloro-2-chloromethylimidazo[1,2-*a*]pyridine **1a** (0.5 g, 1.79 mmol, 1 equiv.) was added. The reaction mixture was stirred for 72 h at room temperature. Then, the mixture was slowly poured into an ice-water mixture and extracted three times with dichloromethane. The organic layer was washed five times with brine, dried over MgSO₄, filtered and evaporated. Compound **5a** was obtained, after purification by chromatography on silica gel (eluent: dichloromethane/cyclohexane/diethyl ether 7:2.5:0.5) and recrystallization from acetonitrile as a white solid in 63% yield (0.28 g). mp 140 °C. ¹H NMR (300 MHz, CDCl₃) δ : 2.48 (3H, s), 7.39–7.41 (2H, m), 8.70 (1H, d, *J* = 1.8 Hz). ¹³C NMR (75 MHz, CDCl₃) δ : 14.7 (CH₃), 111.1 (C), 112.0 (CH), 119.5 (C), 122.5 (CH), 127.5 (CH), 141.8 (C), 145.5 (C). LC/MS ESI⁺ *t*_R 1.71 min, (m/z) [M+H]⁺ 245.05/247.04/249.07. HRMS (+ESI): 246.9453 (M + H⁺). Calcd for C₈H₆BrClN₂: 246.9453.

4.1.10. 8-Bromo-6-chloro-2-methyl-3-nitroimidazo[1,2-*a*]pyridine (**5b**)

To a solution of 8-bromo-6-chloro-2-methylimidazo[1,2-*a*]pyridine **5a** (0.3 g, 1.22 mmol, 1 equiv.) in concentrated sulfuric acid (5 mL) cooled by an ice-water bath, nitric acid 65% (500 μ L, 7.3 mmol, 6 equiv.) was added. The reaction mixture was stirred for 30 min at room temperature. Then, the mixture was slowly poured into an ice-water mixture and the desired product precipitated. The yellow solid was collected by filtration, dried under reduced pressure and recrystallized from acetonitrile to give the expected product **5b** in 78% yield (0.28 g). mp 192 °C. ^1H NMR (300 MHz, DMSO-*d*₆) δ : 2.74 (3H, s), 8.36 (1H, d, *J* = 1.8 Hz), 9.34 (1H, d, *J* = 1.8 Hz). ^{13}C NMR (75 MHz, DMSO-*d*₆) δ : 14.0 (CH₃), 111.3 (C), 122.6 (C), 125.2 (CH), 131.2 (C), 133.5 (CH), 140.7 (C), 150.1 (C). LC/MS ESI⁺ *t*_R 2.13 min, (m/z) [M+H]⁺ 289.90/291.90/293.90. HRMS (+ESI): 291.9302 (M + H⁺). Calcd for C₈H₅BrClN₃O₂: 291.9304.

4.1.11. (8-Bromo-6-chloro-3-nitroimidazo[1,2-*a*]pyridin-2-yl)methanol (**6**)

To a solution of copper sulfate pentahydrate (0.77 g, 3.08 mmol, 1 equiv.) in a dimethylsulfoxide/water mixture (7.5/2.5, 80 mL), 8-bromo-6-chloro-2-chloromethyl-3-nitroimidazo[1,2-*a*]pyridine **1b** (1 g, 3.08 mmol, 1 equiv.) was added. The reaction mixture was stirred and heated at 100 °C for 24 h. Then, the mixture was slowly poured into an ice-water mixture with sodium carbonate and extracted three times with dichloromethane. The organic layer was washed five times with brine, dried over MgSO₄, filtered and evaporated. The crude residue was purified by column chromatography on silica gel (eluent: dichloromethane/ethyl acetate 9.5:0.5) and compound **6** was isolated as a white solid in 32% yield (0.3 g). mp 202 °C. ^1H NMR (300 MHz, DMSO-*d*₆) δ : 4.92 (2H, d, *J* = 6.3 Hz), 5.57 (1H, t, *J* = 6.3 Hz), 8.38 (1H, d, *J* = 1.8 Hz), 9.36 (1H, d, *J* = 1.8 Hz). ^{13}C NMR (75 MHz, DMSO-*d*₆) δ : 58.3 (CH₂), 111.9 (C), 122.9 (C), 125.2 (CH), 129.7 (C), 133.6 (CH), 141.0 (C), 153.2 (C). LC/MS ESI⁺ *t*_R 1.01 min, (m/z) [M+H]⁺ 305.84/307.83/309.91. HRMS (+ESI): 307.9255 (M + H⁺). Calcd for C₈H₅BrClN₃O₃: 307.9253.

4.1.12. 8-Bromo-6-chloro-3-nitro-2-(phenylthiomethyl)imidazo[1,2-*a*]pyridine (**7**)

To a sealed 20 mL flask containing a solution of NaH 60% (0.07 g, 0.98 mmol, 1.1 equiv.) in dimethylsulfoxide (3 mL), thiophenol (0.17 g, 1.54 mmol, 1 equiv.) was added under N₂ atmosphere. The reaction mixture was stirred for 30 min at room temperature. Then, a solution of 8-bromo-6-chloro-2-chloromethyl-3-nitroimidazo[1,2-*a*]pyridine **1b** (0.5 g, 1.54 mmol, 1 equiv.) in dimethylsulfoxide was injected. The reaction mixture was stirred at room temperature for 45 min. Then, the mixture was slowly poured into an ice-water mixture and extracted three times with dichloromethane. The organic layer was washed five times with brine, dried over MgSO₄, filtered and evaporated. The crude residue was purified by column chromatography on silica gel (eluent: dichloromethane/cyclohexane 6:4) and compound **7** was isolated as a yellow solid in 28% yield (0.17 g). mp 136 °C. ¹H NMR (250 MHz, CDCl₃) δ: 4.66 (2H, s), 7.19–7.31 (3H, m), 7.45–7.48 (2H, m), 7.86 (1H, d, *J* = 1.7 Hz), 9.46 (1H, d, *J* = 1.1 Hz). ¹³C NMR (62.5 MHz, CDCl₃) δ: 33.4 (CH₂), 112.9 (C), 124.7 (C), 124.9 (CH), 127.3 (CH), 129.1 (2CH), 131.0 (2CH), 131.9 (C), 133.9 (CH), 134.8 (C), 141.0 (C), 150.5 (C). LC/MS ESI⁺ t_R 4.01 min, (m/z) [M+H]⁺ 398.81/399.84. HRMS (+ESI): 399.9336 (M + H⁺). Calcd for C₁₄H₉BrClN₃O₂S: 399.9338.

4.1.13. General procedure for the preparation of sulfone derivatives from the 8-bromo-6-chloro-2-chloromethyl-3-nitroimidazo[1,2-*a*]pyridine (**1b**) :

To a 20 mL flask containing a solution of 8-bromo-6-chloro-2-chloromethyl-3-nitroimidazo[1,2-*a*]pyridine **1b** (0.8 g, 2.46 mmol, 1 equiv.) in a water/ethanol mixture (1:1, 12 mL), sodium bicarbonate (0.42 g, 4.92 mmol, 2 equiv.), sodium sulfite (0.62 g, 4.92 mmol, 2 equiv.) and the appropriate sulfonyl chloride (4.92 mmol, 2 equiv.) were added. The flask was sealed and the mixture was heated at 120 °C under microwave irradiation until complete disappearance of the starting material (as monitored by LC/MS or TLC). Water was then added and the mixture was extracted three times with dichloromethane. The organic layer was dried over MgSO₄, filtered and evaporated. The crude residue was purified by column chromatography on silica gel and recrystallized from the appropriate solvent, affording compounds **8** to **10**.

4.1.13.1. 8-Bromo-6-chloro-2-(methylsulfonylmethyl)-3-nitroimidazo[1,2-*a*]pyridine (8)

Compound **8** was obtained after purification by chromatography (eluent: dichloromethane/ethyl acetate 9:1) and recrystallization from propan-2-ol as a pale brown solid in 47% yield (0.43 g). mp 233 °C. ¹H NMR (400 MHz, CDCl₃) δ: 3.20 (3H, t, *J* = 0.9 Hz), 5.09 (2H, q, *J* = 0.9 Hz), 7.96 (1H, d, *J* = 1.8 Hz), 9.51 (1H, d, *J* = 1.8 Hz). ¹³C NMR (100 MHz, CDCl₃) δ: 41.9 (CH₃), 54.9 (CH₂), 113.3 (C), 125.0 (CH), 125.6 (C), 131.1 (C), 134.5 (CH), 140.3 (C), 141.3 (C). LC/MS ESI⁺ t_R 0.86 min, (m/z) [M+H]⁺ 367.76/369.89/370.94. HRMS (+ESI): 369.9077 (M + H⁺). Calcd for C₉H₇BrClN₃O₄S: 369.9079.

4.1.13.2. 8-Bromo-6-chloro-2-(cyclohexylsulfonylmethyl)-3-nitroimidazo[1,2-*a*]pyridine (9)

Compound **9** was obtained after purification by chromatography (eluent: dichloromethane) and recrystallization from acetonitrile as a yellow solid in 29% yield (0.31 g). mp 214 °C. ¹H NMR (400 MHz, CDCl₃) δ: 1.22–1.40 (3H, m), 1.60–1.77 (3H, m), 1.96–2.01 (2H, m), 2.29–2.33 (2H, m), 3.28 (1H, tt, *J* = 3.4 and 12.2 Hz), 5.02 (2H, s), 7.92 (1H, d, *J* = 1.8 Hz), 9.47 (1H, d, *J* = 1.8 Hz). ¹³C NMR (100 MHz, CDCl₃) δ: 25.1 (2CH₂), 25.2 (CH₂), 25.3 (2CH₂), 50.1 (CH₂), 61.8 (CH), 113.2 (C), 125.0 (CH), 125.4 (C), 127.0 (C), 134.3 (CH), 140.5 (C), 141.2 (C). LC/MS ESI⁺ t_R 2.92 min, (m/z) [M+H]⁺ 435.79/437.85/437.00. HRMS (+ESI): 435.9723 (M + H⁺). Calcd for C₁₄H₁₅BrClN₃O₄S: 435.9728.

4.1.13.3. 8-Bromo-6-chloro-3-nitro-2-(pyridin-3-ylsulfonylmethyl)imidazo[1,2-*a*]pyridine (10)

Compound **10** was obtained after purification by chromatography (eluent: dichloromethane/cyclohexane/diethyl ether 5:3:2) and recrystallization from acetonitrile as a yellow solid in 21% yield (0.22 g). mp 220 °C. ¹H NMR (400 MHz, CDCl₃) δ: 5.21 (2H, s), 7.53–7.56 (1H, m), 7.91 (1H, d, *J* = 1.8 Hz), 8.21 (1H, dt, *J* = 1.7 and 8.1 Hz), 8.90 (1H, bd, *J* = 3.9 Hz),

9.01 (1H, bs), 9.45 (1H, d, $J = 1.8$ Hz). ^{13}C NMR (100 MHz, CDCl_3) δ : 56.9 (CH_2), 113.4 (C), 124.0 (CH), 124.9 (CH), 125.8 (C), 128.3 (C), 134.5 (CH), 135.8 (C), 136.9 (CH), 139.3 (C), 141.2 (C), 149.7 (CH), 154.6 (CH). LC/MS ESI⁺ t_{R} 1.21 min, (m/z) $[\text{M}+\text{H}]^+$ 430.61/432.29/433.31. HRMS (+ESI): 430.9210 (M + H⁺). Calcd for $\text{C}_{13}\text{H}_8\text{BrClN}_4\text{O}_4\text{S}$: 430.9211.

4.1.14. General procedure for the preparation of 8-(4-chlorophenylthio)imidazo[1,2-*a*]pyridine derivatives (11 to 19):

To a sealed 20 mL flask containing NaH 60% (9.4 mg, 0.47 mmol, 1 equiv.) in dimethylsulfoxide (1 mL), 4-chlorothiophenol (68 mg, 0.47 mmol, 1 equiv.) was added under N_2 atmosphere. The reaction mixture was stirred at room temperature for 30 min. Then a solution of the appropriate 8-bromo-3-nitro-imidazo[1,2-*a*]pyridine derivative (0.47 mmol, 1 equiv.) in dimethylsulfoxide (5 mL) was injected. The reaction mixture was stirred at room temperature until complete disappearance of the starting material (as monitored by LC/MS or TLC). The reaction mixture was then poured into an ice-water mixture. The mixture was extracted three times with dichloromethane, then the organic layer was washed five times with brine, dried over MgSO_4 , filtered and evaporated. The crude residue was purified by column chromatography on silica gel and/or recrystallized from the appropriate solvent, affording compounds **11** to **19**.

4.1.14.1. 8-[4-(Chlorophenyl)thio]-6-methyl-3-nitro-2-(phenylsulfonylmethyl)imidazo[1,2-*a*]pyridine (11)

Compound **11** was obtained after purification by chromatography (eluent: petroleum ether/ethyl acetate 7:3) and recrystallization from acetonitrile as a yellow solid in 90% yield (0.18 g). mp 184 °C. ^1H NMR (200 MHz, CDCl_3) δ : 2.34 (3H, s), 5.17 (2H, s), 6.77 (1H, d, $J = 1.1$ Hz), 7.44–7.48 (2H, m), 7.51–7.57 (4H, m), 7.64–7.70 (1H, m), 7.87–7.90 (2H, m), 8.96–8.97 (1H, m). ^{13}C NMR (50 MHz, CDCl_3) δ : 19.0 (CH_3), 56.9 (CH_2), 122.7 (C), 127.5 (C), 127.8 (CH), 128.7 (2CH), 129.2 (C), 129.3 (2CH), 130.5 (CH), 130.6 (2CH), 131.1 (C), 134.2 (CH), 136.6 (C), 136.7 (2CH), 138.7

(C), 139.4 (C), 141.0 (C). LC/MS ESI⁺ t_R 3.80 min, (m/z) [M+H]⁺ 473.83/475.84. HRMS (+ESI): 474.0340 (M + H⁺). Calcd for C₂₁H₁₆ClN₃O₄S₂: 474.0344.

4.1.14.2. 8-[4-(Chlorophenyl)thio]-3-nitro-2-(phenylsulfonylmethyl)-6-(trifluoromethyl)imidazo[1,2-*a*]pyridine (12)

Compound **12** was obtained after recrystallization from propan-2-ol as a yellow solid in 70% yield (0.17 g). mp 191 °C. ¹H NMR (250 MHz, CDCl₃) δ: 5.18 (2H, s), 6.91 (1H, d, *J* = 1.2 Hz), 7.47–7.63 (6H, m), 7.71 (1H, t, *J* = 7.4 Hz), 7.90 (2H, dd, *J* = 1.4 and 7.2 Hz), 9.44 (1H, s). ¹³C NMR (62.5 MHz, CDCl₃) δ: 56.7 (CH₂), 120.5 (CH, d, *J* = 2.7 Hz), 121.6 (C, q, *J* = 34.8 Hz), 122.5 (CH, d, *J* = 5.6 Hz), 122.5 (C, q, *J* = 272.8 Hz), 125.6 (CH), 128.6 (2CH), 129.4 (2CH), 131.0 (C), 132.0 (2CH), 134.0 (C), 134.5 (C), 137.1 (2CH), 137.6 (C), 139.2 (C), 139.9 (C), 141.4 (C). LC/MS ESI⁺ t_R 4.24 min, (m/z) [M+H]⁺ 528.11/529.15. HRMS (+ESI): 528.0061 (M + H⁺). Calcd for C₂₁H₁₃ClF₃N₃O₄S₂: 528.0061.

4.1.14.3. 6-Chloro-8-[4-(chlorophenyl)thio]-3-nitroimidazo[1,2-*a*]pyridine (13)

Compound **13** was obtained after purification by chromatography (eluent: dichloromethane/cyclohexane 7:3) and recrystallization from acetonitrile as a yellow solid in 69% yield (0.11 g). mp 192 °C. ¹H NMR (400 MHz, CDCl₃) δ: 6.78 (1H, d, *J* = 1.8 Hz), 7.49–7.53 (2H, m), 7.57–7.60 (2H, m), 8.59 (1H, s), 9.20 (1H, d, *J* = 1.8 Hz). ¹³C NMR (100 MHz, CDCl₃) δ: 121.6 (CH), 125.7 (CH), 125.8 (C), 126.2 (C), 130.9 (2CH), 133.0 (C), 133.3 (C), 137.0 (2CH), 137.4 (C), 137.5 (CH), 142.1 (C). LC/MS ESI⁺ t_R 4.10 min, (m/z) [M+H]⁺ 340.10/341.11/342.08. HRMS (+ESI): 339.9705 (M + H⁺). Calcd for C₁₃H₇Cl₂N₃O₂S: 339.9709.

4.1.14.4. 6-Chloro-8-[4-(chlorophenyl)thio]-2-methyl-3-nitroimidazo[1,2-*a*]pyridine (14)

Compound **14** was obtained after purification by chromatography (eluent: dichloromethane) and recrystallization from acetonitrile as a yellow solid in 75% yield (0.13 g). mp 199 °C. ¹H NMR (400 MHz, CDCl₃) δ: 2.89 (3H, s), 6.75 (1H, d, *J* = 1.8 Hz), 7.48–7.60 (4H, m), 9.23 (1H, d, *J* =

1.8 Hz). ^{13}C NMR (100 MHz, CDCl_3) δ : 17.5 (CH_3), 122.2 (CH), 124.8 (C), 125.9 (CH), 126.4 (C), 130.9 (2CH), 131.2 (C), 131.6 (C), 137.0 (2CH), 137.3 (C), 140.0 (C), 150.5 (C). LC/MS ESI⁺ t_{R} 4.50 min, (m/z) $[\text{M}+\text{H}]^+$ 354.08/355.19/356.31. HRMS (+ESI): 353.9864 (M + H⁺). Calcd for $\text{C}_{14}\text{H}_9\text{Cl}_2\text{N}_3\text{O}_2\text{S}$: 353.9865.

4.1.14.5. {6-Chloro-8-[4-(chlorophenyl)thio]-3-nitroimidazo[1,2-*a*]pyridin-2-yl}methanol (15)

Compound **15** was obtained after purification by chromatography (eluent: dichloromethane/methanol 9.8:0.2) as a pale yellow solid in 40% yield (70 mg). mp 227 °C. ^1H NMR (400 MHz, $\text{DMSO-}d_6$) δ : 4.92 (2H, s), 5.54 (1H, sl), 6.99 (1H, d, $J = 1.8$ Hz), 7.61–7.68 (4H, m), 9.17 (1H, d, $J = 1.8$ Hz). ^{13}C NMR (100 MHz, $\text{DMSO-}d_6$) δ : 58.2 (CH_2), 122.9 (CH), 123.3 (C), 126.6 (CH), 127.2 (C), 129.4 (C), 129.7 (C), 130.5 (2CH), 135.1 (C), 136.2 (2CH), 140.0 (C), 152.5 (C). LC/MS ESI⁺ t_{R} 3.68 min, (m/z) $[\text{M}+\text{H}]^+$ 369.86/371.12/372.06. HRMS (+ESI): 369.9811 (M + H⁺). Calcd for $\text{C}_{14}\text{H}_9\text{Cl}_2\text{N}_3\text{O}_3\text{S}$: 369.9814.

4.1.14.6. 6-Chloro-8-[4-(chlorophenyl)thio]-3-nitro-2-(phenylthiomethyl)imidazo[1,2-*a*]pyridine (16)

Compound **16** was obtained after purification by chromatography (eluent: petroleum ether/dichloromethane 5.5:4.5) as a yellow solid in 21% yield (46 mg). mp 142 °C. ^1H NMR (200 MHz, CDCl_3) δ : 4.67 (2H, s), 6.76 (1H, d, $J = 1.8$ Hz), 7.22–7.25 (1H, m), 7.29–7.33 (1H, m), 7.48–7.58 (7H, m), 9.21 (1H, d, $J = 1.8$ Hz). ^{13}C NMR (50 MHz, CDCl_3) δ : 33.3 (CH_2), 122.1 (C), 125.4 (C), 126.2 (CH), 126.3 (C), 127.1 (CH), 129.1 (2CH), 130.6 (2CH), 130.9 (2CH), 132.3 (C), 135.2 (C), 135.9 (CH), 137.0 (2CH), 137.3 (C), 139.8 (C), 149.6 (C). LC/MS ESI⁺ t_{R} 5.36 min, (m/z) $[\text{M}+\text{H}]^+$ 461.81/463.92. HRMS (+ESI): 461.9897 (M + H⁺). Calcd for $\text{C}_{20}\text{H}_{13}\text{Cl}_2\text{N}_3\text{O}_2\text{S}_2$: 461.9899.

4.1.14.7. 6-Chloro-8-[4-(chlorophenyl)thio]-2-(methylsulfonylmethyl)-3-nitroimidazo[1,2-*a*]pyridine (17)

Compound **17** was obtained after purification by chromatography (eluent: dichloromethane) and recrystallization from acetonitrile as a beige solid in 46% yield (93 mg). mp 213 °C. ¹H NMR (400 MHz, DMSO-*d*₆) δ: 3.07 (3H, s), 5.11 (2H, q, *J* = 0.8 Hz), 7.18 (1H, d, *J* = 1.8 Hz), 7.58–7.67 (4H, m), 9.22 (1H, d, *J* = 1.8 Hz). ¹³C NMR (100 MHz, DMSO-*d*₆) δ: 40.9 (CH₃), 54.1 (CH₂), 123.5 (CH), 123.9 (C), 127.5 (C), 128.0 (CH), 129.3 (C), 130.3 (2CH), 131.5 (C), 134.9 (C), 135.7 (2CH), 139.4 (C), 140.0 (C). LC/MS ESI⁺ t_R 3.42 min, (m/z) [M+H]⁺ 432.70/433.72/434.89. HRMS (+ESI): 431.9640 (M + H⁺). Calcd for C₁₅H₁₁Cl₂N₃O₄S₂: 431.9641.

4.1.14.8. 6-Chloro-8-[4-(chlorophenyl)thio]-2-(cyclohexylsulfonylmethyl)-3-nitroimidazo[1,2-*a*]pyridine (18)

Compound **18** was obtained after purification by chromatography (eluent: dichloromethane) and recrystallization from cyclohexane as a brown solid in 47% yield (0.11 g). mp 82 °C. ¹H NMR (400 MHz, CDCl₃) δ: 1.21–1.39 (3H, m), 1.61–1.78 (3H, m), 1.97–2.01 (2H, m), 2.31–2.34 (2H, m), 3.31 (1H, tt, *J* = 3.4 and 12.1 Hz), 5.02 (2H, s), 6.79 (1H, d, *J* = 1.8 Hz), 7.50–7.59 (4H, m), 9.22 (1H, d, *J* = 1.8 Hz). ¹³C NMR (100 MHz, CDCl₃) δ: 25.1 (2CH₂), 25.2 (CH₂), 25.3 (2CH₂), 50.0 (CH₂), 61.6 (CH), 113.1 (C), 122.0 (CH), 126.0 (C), 126.3 (CH), 130.1 (C), 131.0 (2CH), 132.8 (C), 137.0 (2CH), 137.5 (C), 139.5 (C), 140.0 (C). LC/MS ESI⁺ t_R 4.57 min, (m/z) [M+H]⁺ 499.81/501.85/503.88. HRMS (+ESI): 500.0271 (M + H⁺). Calcd for C₂₀H₁₉Cl₂N₃O₄S₂: 500.0267.

4.1.14.9. 6-Chloro-8-[4-(chlorophenyl)thio]-3-nitro-2-(pyridin-3-ylsulfonylmethyl)imidazo[1,2-*a*]pyridine (19)

Compound **19** was obtained after purification by chromatography (eluent: dichloromethane) and recrystallization from acetonitrile as a yellow solid in 20% yield (47 mg). mp 176 °C. ¹H NMR (400 MHz, CDCl₃) δ: 5.21 (2H, s), 6.74 (1H, d, *J* = 1.7 Hz), 7.50–7.59 (5H, m), 8.23 (1H, dt, *J* = 1.7 and 7.9 Hz), 8.91 (1H, d, *J* = 4.1 Hz), 9.01 (1H, s), 9.17 (1H, d, *J* = 1.7 Hz). ¹³C NMR (100

MHz, CDCl₃) δ : 56.9 (CH₂), 121.8 (CH), 123.9 (CH), 125.6 (C), 126.1 (CH), 126.4 (C), 131.0 (2CH), 132.0 (C), 133.4 (C), 135.8 (C), 136.8 (CH), 137.2 (2CH), 137.6 (C), 138.4 (C), 139.9 (C), 149.8 (CH), 154.8 (CH). LC/MS ESI⁺ t_R 3.63 min, (m/z) [M+H]⁺ 494.77/496.71. HRMS (+ESI): 494.9750 (M + H⁺). Calcd for C₁₉H₁₂Cl₂N₄O₄S₂: 494.9750.

4.1.15. General procedure for the preparation of 8-arylamino-imidazo[1,2-*a*]pyridine derivatives (**20** to **22**):

A mixture of 8-bromo-6-chloro-3-nitro-2-(phenylsulfonylmethyl)imidazo[1,2-*a*]pyridine **1c** (400 mg, 0.93 mmol, 1 equiv.), palladium diacetate (17 mg, 0.07 mmol, 0.08 equiv.), potassium carbonate (0.23 g, 1.7 mmol, 1.8 equiv.), *rac*-BINAP (87 mg, 0.14 mmol, 0.15 equiv.) and appropriate aniline (1.1 mmol, 1.2 equiv.) in toluene (12 mL) under N₂ atmosphere was heated at 140 °C under microwave irradiation until complete disappearance of the starting material (as monitored by LC/MS or TLC). Water was then added and the mixture was extracted three times with dichloromethane. The organic layer was washed three times with water, dried over MgSO₄, filtered and evaporated. The crude residue was purified by column chromatography on silica gel with 0.5% triethylamine and recrystallized from the appropriate solvent, affording compounds **20** to **22**.

4.1.15.1. 6-Chloro-3-nitro-*N*-phenyl-2-(phenylsulfonylmethyl)imidazo[1,2-*a*]pyridin-8-amine (**20**)

Compound **20** was obtained after purification by chromatography (eluent: dichloromethane/cyclohexane 7:3) and recrystallization from propan-2-ol as an orange solid in 50% yield (0.21 g). mp 254 °C. ¹H NMR (400 MHz, CDCl₃) δ : 5.18 (2H, s), 7.12–7.16 (2H, m), 7.40–7.42 (4H, m), 7.60–7.64 (2H, m), 7.74–7.80 (3H, m), 8.72 (1H, d, *J* = 1.3 Hz), 9.09 (1H, bs). ¹³C NMR (100 MHz, CDCl₃) δ : 56.4 (CH₂), 107.6 (CH), 114.6 (CH), 121.9 (2CH), 124.0 (CH), 125.6 (C), 128.0 (2CH), 129.4 (4CH), 131.5 (C), 134.3 (CH), 134.5 (C), 136.3 (C), 136.9 (C), 138.8 (C), 139.4 (C). LC/MS ESI⁺ t_R 4.08 min, (m/z) [M+H]⁺ 442.91/444.90. HRMS (+ESI): 443.0577 (M + H⁺). Calcd for C₂₀H₁₅ClN₄O₄S: 443.0575.

4.1.15.2. 6-Chloro-*N*-(4-chlorophenyl)-3-nitro-2-(phenylsulfonylmethyl)imidazo[1,2-*a*]pyridin-8-amine (21)

Compound **21** was obtained after purification by chromatography (eluent: dichloromethane) and recrystallization from propan-2-ol as an orange solid in 52% yield (0.23 g). mp 255 °C. ¹H NMR (400 MHz, DMSO-*d*₆) δ: δ 5.17 (2H, s), 7.18–7.20 (1H, m), 7.39–7.48 (4H, m), 7.59–7.63 (2H, m), 7.74–7.79 (3H, m), 7.76–7.76 (1H, m), 9.23 (1H, bs). ¹³C NMR (100 MHz, DMSO-*d*₆) δ: 56.4 (CH₂), 108.5 (CH), 115.2 (CH), 123.1 (2CH), 125.5 (C), 127.3 (C), 128.0 (2CH), 129.3 (2CH), 129.4 (2CH), 130.6 (C), 131.5 (C), 134.0 (C), 134.3 (CH), 137.0 (C), 138.7 (C), 138.8 (C). LC/MS ESI⁺ t_R 4.99 min, (m/z) [M+H]⁺ 476.69/478.60. HRMS (+ESI): 477.0186 (M + H⁺). Calcd for C₂₀H₁₄Cl₂N₄O₄S: 477.0186.

4.1.15.3. 6-Chloro-*N*-(4-methoxyphenyl)-3-nitro-2-(phenylsulfonylmethyl)imidazo[1,2-*a*]pyridin-8-amine (22)

Compound **22** was obtained after purification by chromatography (eluent: dichloromethane/cyclohexane 9:1) and recrystallization from propan-2-ol as a red solid in 42% yield (0.19 g). mp 228 °C. ¹H NMR (400 MHz, CDCl₃) δ: 3.78 (3H, s), 5.17 (2H, s), 6.81 (1H, d, *J* = 1.4 Hz), 6.99–7.01 (2H, m), 7.30–7.32 (2H, m), 7.60–7.64 (2H, m), 7.74–7.80 (3H, m), 8.64 (1H, d, *J* = 1.4 Hz), 8.93 (1H, s). ¹³C NMR (100 MHz, CDCl₃) δ: 55.3 (CH₃), 56.4 (CH₂), 106.0 (CH), 113.6 (CH), 114.7 (2CH), 125.0 (2CH), 125.8 (C), 128.0 (2CH), 129.4 (2CH), 131.4 (C), 131.7 (C), 134.3 (CH), 135.9 (C), 136.0 (C), 136.8 (C), 138.8 (C), 156.5 (C). LC/MS ESI⁺ t_R 4.62 min, (m/z) [M+H]⁺ 472.88/474.74. HRMS (+ESI): 473.0680 (M + H⁺). Calcd for C₂₁H₁₇ClN₄O₅S: 473.0681.

4.1.16. 6-Chloro-8-(4-chlorophenylselenanyl)-3-nitro-2-(phenylsulfonylmethyl)imidazo[1,2-*a*]pyridine (23)

To a solution of 1,2-bis(4-chlorophenyl)diselenide [24] (0.4 g, 1.05 mmol, 1 equiv.) in PEG-400 (4 mL) under N₂ atmosphere, sodium borohydride (0.16 g, 4.2 mmol, 4 equiv.) was added. The reaction mixture was stirred 1 h at 60 °C. 8-bromo-6-chloro-3-nitro-2-(phenylsulfonylmethyl)imidazo[1,2-*a*]pyridine **1c** (0.9 g, 2.1 mmol, 2 equiv.) was then introduced. The resulting mixture was diluted with H₂O and acidified with 1 N hydrochloric acid. The mixture

was extracted three times with dichloromethane, dried over MgSO_4 , filtered and evaporated. The crude residue was purified by column chromatography on silica gel (eluent: dichloromethane) as a yellow solid in 9% yield (0.11 g). mp 209 °C. ^1H NMR (250 MHz, CDCl_3) δ : 5.15 (2H, s), 6.87 (1H, d, $J = 1.7$ Hz), 7.42-7.75 (7H, m), 7.90 (2H, d, $J = 7.3$ Hz), 9.20 (1H, d, $J = 1.7$ Hz). ^{13}C NMR (63 MHz, CDCl_3) δ : 56.7 (CH_2), 122.2 (CH), 122.5 (C), 126.3 (C), 128.6 (C), 128.7 (2CH), 128.9 (C), 129.4 (2CH), 131.0 (2CH), 131.3 (CH), 134.4 (C), 137.3 (CH), 138.6 (2CH), 139.1 (C), 139.3 (C), 140.7 (C). LC/MS ESI⁺ t_{R} 4.31 min, (m/z) $[\text{M}+\text{H}]^+$ 541.68/543.53/546.10. HRMS (+ESI): 540.9169 (M + H⁺). Calcd for $\text{C}_{20}\text{H}_{13}\text{Cl}_2\text{N}_3\text{O}_4\text{SSe}$: 540.9171.

4.1.17. 8-Bromo-6-chloro-2-(methylthiomethyl)-3-nitroimidazo[1,2-*a*]pyridine (24)

To a solution of 8-bromo-6-chloro-2-chloromethyl-3-nitroimidazo[1,2-*a*]pyridine **1b** (0.8 g, 2.46 mmol, 1 equiv.) in DMSO (10 mL), a solution of sodium thiomethoxide (0.17 g, 2.46 mmol, 1 equiv.) in DMSO (5 mL) was added dropwise. The reaction mixture was stirred for 45 min at room temperature. Then, the mixture was slowly poured into an ice-water mixture and the desired product precipitated. The yellow solid was collected by filtration, dried under reduced pressure and purified by column chromatography on silica gel (eluent: dichloromethane/cyclohexane 5:5) as a pale yellow solid in 52% yield (0.43 g). mp 186 °C. ^1H NMR (400 MHz, $\text{DMSO-}d_6$) δ : 2.13 (3H, s), 4.13 (2H, s), 8.40 (1H, d, $J = 1.8$ Hz), 9.37 (1H, d, $J = 1.8$ Hz). ^{13}C NMR (100 MHz, $\text{DMSO-}d_6$) δ : 14.9 (CH_3), 31.1 (CH_2), 111.7 (C), 123.0 (CH), 125.5 (C), 130.0 (C), 133.8 (CH), 140.7 (C), 150.4 (C). LC/MS ESI⁺ t_{R} 2.76 min, (m/z) $[\text{M}+\text{H}]^+$ 334.64/337.82/339.91. HRMS (+ESI): 337.9182 (M + H⁺). Calcd for $\text{C}_9\text{H}_7\text{BrClN}_3\text{O}_2\text{S}$: 337.9181.

4.1.18. 8-Bromo-6-chloro-2-(methylsulfinylmethyl)-3-nitroimidazo[1,2-*a*]pyridine

(25)

To a solution of 8-bromo-6-chloro-2-(methylthiomethyl)-3-nitroimidazo[1,2-*a*]pyridine **24** (0.4 g, 1.19 mmol, 1 equiv.) in dichloromethane (40 mL) cooled by an ice-water bath, mCPBA (~70%) (0.29 g, 1.19 mmol, 1 equiv.) was added. The reaction mixture was stirred for 1 h at 0 °C. Then,

the mixture was washed three times with H₂O, dried over MgSO₄, filtered and evaporated. The crude residue was purified by column chromatography on silica gel (eluent: dichloromethane/ethyl acetate 8:2) as a yellow solid in 36% yield (0.15 g). mp 164 °C. ¹H NMR (400 MHz, DMSO-*d*₆) δ: 2.70 (3H, s), 4.55-4.81 (2H, m), 8.42 (1H, d, *J* = 1.8 Hz), 9.38 (1H, d, *J* = 1.8 Hz). ¹³C NMR (100 MHz, DMSO-*d*₆) δ: 38.6 (CH₃), 53.3 (CH₂), 111.8 (C), 123.3 (CH), 125.4 (C), 132.0 (C), 134.0 (CH), 141.0 (C), 142.7 (C). LC/MS ESI⁺ t_R 0.84 min, (m/z) [M+H]⁺ 351.83/353.92/355.94. HRMS (+ESI): 353.9127 (M + H⁺). Calcd for C₉H₇BrClN₃O₃S: 353.9130.

4.1.19. 8-Bromo-6-chloro-2-(methylsulfonylmethyl)imidazo[1,2-*a*]pyridin-3-amine

(26)

To a solution of 8-bromo-6-chloro-2-(methylsulfonylmethyl)-3-nitroimidazo[1,2-*a*]pyridine **8** (0.2 g, 0.54 mmol, 1 equiv.) in acetic acid (30 mL), iron powder (0.3 g, 5.4 mmol, 10 equiv.) was added. The reaction mixture was stirred and heated under reflux for 30 min. The mixture was then filtered through celite and the solvent was removed *in vacuo*. The resulting residue was diluted with H₂O and basified with sat. aq. NaHCO₃. The mixture was extracted three times with dichloromethane, dried over MgSO₄, filtered and evaporated. The crude residue was purified by column chromatography on silica gel (eluent: dichloromethane/diethyl ether 6:4) as a yellow solid in 40% yield (0.07 g). mp 215 °C. ¹H NMR (250 MHz, DMSO) δ: 3.02 (3H, s), 4.62 (2H, s), 5.62 (2H, s), 7.50 (1H, d, *J* = 1.7 Hz), 8.33 (1H, d, *J* = 1.7 Hz). ¹³C NMR (62.5 MHz, DMSO) δ: 40.1 (CH₃), 52.7 (CH₂), 110.8 (C), 117.4 (CH), 117.6 (C), 119.9 (C), 123.7 (CH), 133.0 (C), 134.2 (C). LC/MS ESI⁺ t_R 1.03 min, (m/z) [M+H]⁺ 337.90/339.92/341.95. HRMS (+ESI): 339.9336 (M + H⁺). Calcd for C₉H₉N₃O₂SBrCl: 339.9337.

4.2. Electrochemistry

Voltammetric measurements were carried out with a potentiostat Autolab PGSTAT100 (ECO Chemie, The Netherlands) controlled by GPES 4.09 software. Experiments were performed at

room temperature in a homemade airtight three-electrode cell connected to a vacuum/argon line. The reference electrode consisted of a saturated calomel electrode (SCE) separated from the solution by a bridge compartment. The counter electrode was a platinum wire of 1 cm² apparent surface. The working electrode was GC microdisk (1.0 mm of diameter – Bio-logic SAS). The supporting electrolyte (nBu₄N)[PF₆] (Fluka, 99% puriss electrochemical grade) and the solvent DMSO (Sigma-Aldrich puriss p.a. dried <0.02% water) were used as received and simply degassed under argon. The solutions used during the electrochemical studies were typically 10⁻³ M in compound and 0.1 M in supporting electrolyte. Before each measurement, the solutions were degassed by bubbling Ar and the working electrode was polished with a polishing machine (Presi P230). Under these experimental conditions employed in this work, the half-wave potential ($E_{1/2}$) of the ferrocene Fc⁺/Fc couple in DMSO was $E_{1/2} = 0.45$ V vs SCE. Experimental peak potentials have been measured versus SCE and converted to NHE by adding 0.241 V.

4.3. Biology

4.3.1. Antileishmanial activity against *L. donovani* promastigotes

Leishmania species used in this study were *L. donovani* (MHOM/IN/00/DEVI) purchased from CNR Leishmania (Montpellier, France). *Leishmania* promastigotes forms were grown in Schneider's Drosophila medium (Life Technologies, Saint-Aubin, France) supplemented with 100 U/mL penicillin, 100 µg/mL streptomycin, 2 mM L-glutamine and 20% FCS (Life Technologies, Saint-Aubin, France) at 27 °C. The *in vitro* evaluation of the antileishmanial activity on promastigote forms of the tested compound was carried out by an MTT assay according to the Mosmann protocol [29] with some modifications. Briefly, promastigotes in log-phase were incubated at an average density of 10⁶ parasites/mL in sterile 96-well plates with various concentrations of compound dissolved in DMSO (final concentration less than 0.5% v/v), in duplicate. Appropriate controls treated by DMSO, miltefosine, amphotericin B, fexinidazole and

doxorubicin (reference drugs purchased from Sigma-Aldrich, Saint-Louis, Missouri, USA) were added to each set of experiments. After a 72h incubation period at 27 °C, parasitic metabolic activity was determined. Each plate-well was then microscope-analyzed for detecting possible precipitate formation. 20 µL of MTT (3-(4,5-dimethylthiazol-2-yl)-2,5-diphenyltetrazolium bromide) (Sigma-Aldrich, Saint-Louis, Missouri, USA) solution (5 mg/mL in PBS) were added to each well followed and incubated 4 h at 27 °C. The enzyme reaction was then stopped by addition of 100 µL of 50% isopropanol – 10% sodium dodecyl sulfate. Plates were shaken vigorously at 300 rpm for 10 min. The absorbance was finally measured at 570 nm in a BIO-TEK Elx808 (Biotek, Colmar, France) absorbance microplate reader. Inhibitory concentration 50% (EC₅₀) was defined as the concentration of drug required to inhibit by 50% the metabolic activity of *Leishmanial* promastigotes forms compared to the control. EC₅₀ were calculated by non-linear regression analysis processed dose-response curves, using TableCurve 2D V5.0 software. EC₅₀ values represent the mean value calculated from at least three independent experiments.

4.3.2. Antileishmanial activity on *L. infantum* axenic amastigotes [29]

L. infantum promastigotes (MHOM/MA/67/ITMAP-263, CNR Leishmania, Montpellier, France, expressing luciferase activity) were cultivated in RPMI 1640 medium supplemented with 10% foetal calf serum (FCS), 2 mM L-glutamine and antibiotics (100 U/mL penicillin and 100 µg/mL streptomycin) and harvested in logarithmic phase of growth by centrifugation at 900 g for 10 min. The supernatant was removed carefully and was replaced by the same volume of RPMI 1640 complete medium at pH 5.4 and incubated for 24 h at 24 °C. The acidified promastigotes were then incubated for 24 h at 37 °C in a ventilated flask to transform promastigotes into axenic amastigotes. The amastigote stage was checked both by electron microscopy (short flagellum with small bulbous tip extending beyond a spherical cell body) and RT-PCR for confirming the overexpression of ATG8 and amastin genes in amastigotes, compared to promastigotes. The effects of the tested compounds on the growth of *L. infantum* axenic amastigotes were assessed as

follows. *L. infantum* amastigotes were incubated at a density of 2×10^6 parasites/mL in sterile 96-well plates with various concentrations of compounds dissolved in DMSO (final concentration less than 0.5% v/v), in duplicate. Appropriate controls DMSO, amphotericin B, miltefosine and fexinidazole (reference drugs purchased from Sigma Aldrich) were added to each set of experiments. After a 48 h incubation period at 37 °C, each plate-well was then microscopically-examined to detect any precipitate formation. To estimate the luciferase activity of axenic amastigotes, 80 µL of each well were transferred to white 96-well plates, Steady Glow® reagent (Promega) was added according to manufacturer's instructions, and plates were incubated for 2 min. The luminescence was measured in Microbeta Luminescence Counter (PerkinElmer). Efficient concentration 50% (EC₅₀) was defined as the concentration of drug required to inhibit by 50% the metabolic activity of *L. infantum* amastigotes compared to control. EC₅₀ values were calculated by non-linear regression analysis processed on dose response curves, using TableCurve 2D V5 software. EC₅₀ values represent the mean of three independent experiments.

4.3.3. Antileishmanial activity on *L. donovani* intracellular amastigotes

4.3.3.1. Cells culture

The undifferentiated THP1 (ATCC) human monocyte cells were grown in RPMI 1640 medium (Life Technologies, Saint-Aubin, France) supplemented with 10% FCS (Life Technologies, Saint-Aubin, France), 100 U/mL penicillin, 100 µg/mL streptomycin and 2 mM L-glutamine at 37 °C, 5% CO₂. The culture was maintained between $3 \cdot 10^5$ and $1 \cdot 10^6$ cells/ml.

4.3.3.2. Antileishmanial evaluation

The *in vitro* evaluation of the antileishmanial activity on intracellular amastigotes forms of the tested compound was assessed according to the da Luz *et al* protocol [30] with some modifications. Briefly, 400 µL of THP-1 cells with Phorbol 12-Myristate 13-Acetate (final concentration 50 ng/ml) were seeded in sterile chamber-slides at an average density of 5×10^4 cells/ml and incubated for 48 h at 37 °C, 5 µ CO₂. Leishmanial promastigotes forms were centrifuged at 3000

rpm for 10 min and the supernatant replaced by the same volume of Schneider 20% FCS pH 5.4 and incubated for 24 hours at 27 °C. Differentiated THP-1 cells were then infected by acidified promastigotes with an infection ratio of ten parasites for one macrophage and incubated for 24 hours at 37 °C, 5% CO₂. Then, in duplicate, the medium containing various concentrations of tested-compounds was added (final DMSO concentration being inferior to 0.5% v/v). Appropriate control treated with or without solvent (DMSO), and various concentration of miltefosine, Amphotericin B and Fexinidazole (reference drugs purchased from Sigma-Aldrich, Saint-Louis, Missouri, USA) were added to each set of experiments. After 120 hours incubation at 37 °C, 5% CO₂, well supernatant was removed. Cells were then fixed with analytical grade methanol and stained with 10% Giemsa (Sigma-Aldrich, Saint-Louis, Missouri, USA). The percentage of infected macrophages in each assay was determined microscopically by counting at least 200 cells in each sample. IC₅₀ was defined as the concentration of drug necessary to produce 50% decrease of infected macrophages compared to the control. IC₅₀ were calculated by non-linear regression analysis processed on dose-response curves, using Table-Curve 2D V5.0 software. IC₅₀ values represent the mean value calculated from at least three independent experiments.

4.3.4. Antitrypanosomal evaluation on *T. b. brucei* BSF trypomastigotes

The effects of the tested compounds on the growth of *T. b. brucei* were assessed by Alamar Blue[®] assay described by Rüz *et al.* [31] *T. b. brucei* AnTat 1.9 (IMTA, Antwerpen, Belgium) was cultured in MEM with Earle's salts, supplemented according to the protocol of Baltz *et al.* [32] with the following modifications: 0.5 mM mercaptoethanol (Sigma Aldrich[®], France), 1.5 mM L-cysteine (Sigma Aldrich[®]), 0.05 mM bathocuproïne sulfate (Sigma Aldrich[®]) and 20% heat-inactivated horse serum (Gibco[®], France), at 37 °C and 5% CO₂. They were incubated at an average density of 2000 parasites/100 µL in sterile 96-wells plates (Fisher[®], France) with various concentrations of compounds dissolved in DMSO, in duplicate. Appropriate controls treated by DMSO on sterile water, suramin, eflornithine and fexinidazole (reference drugs purchased from

Sigma Aldrich, France and Fluorochem, UK) were added to each set of experiments. After a 69 h incubation period at 37 °C, 10 µL of the viability marker Alamar Blue[®] (Fisher, France) was then added to each well, and the plates were incubated for 5 h. The plates were read in a ENSPIRE microplate reader (PerkinElmer) using an excitation wavelength of 530 nm and an emission wavelength of 590 nm. EC₅₀ was defined as the concentration of drug necessary to inhibit by 50% the activity of *T. b. brucei* compared to the control. EC₅₀ were calculated by nonlinear regression analysis processed on dose-response curves, using GraphPad Prism software (USA). EC₅₀ values were calculated from three independent experiments.

4.3.5. Antitrypanosomal activity on *T. brucei* NTR1 over-expressing strain.

Trypanosoma brucei bloodstream-form 'single marker' S427 (T7RPOL TETR NEO) and drug-resistant cell lines were cultured at 37 °C in HMI9-T medium [33] supplemented with 2.5 µg/mL G418 to maintain expression of T7 RNA polymerase and the tetracycline repressor protein. Bloodstream trypanosomes overexpressing the *T. brucei* nitroreductase (NTR1) [34] were grown in medium supplemented with 2.5 µg/mL phleomycin and expression of NTR was induced by the addition of 1 µg/mL tetracycline. Cultures were initiated with 1×10^5 cells/mL and sub-cultured when cell densities approached $1-2 (\times 10^6)/\text{mL}$.

In order to examine the effects of inhibitors on the growth of these parasites, triplicate cultures containing the inhibitor were seeded at 1×10^5 trypanosomes/mL. Cells overexpressing NTR were induced with tetracycline 48 h prior to EC₅₀ analysis. Cell densities were determined after culture for 72 h, as previously described [35]. EC₅₀ values were determined using the following two-parameter equation by non-linear regression using GRAFIT:

where the experimental data were corrected for background cell density and expressed as a percentage of the uninhibited control cell density.

$$y = \frac{100}{1 + \left(\frac{[I]}{EC_{50}} \right)^m}$$

In this equation, [I] represents inhibitor concentration and m is the slope factor.

4.3.6. Cytotoxicity evaluation on HepG2 cell line

HepG2 cell line was maintained at 37 °C, 6% CO₂ with 90% humidity in RPMI supplemented with 10% foetal bovine serum, 1% L-glutamine (200 mM) and penicillin (100 U/mL)/streptomycin (100 mg/mL) (complete RPMI medium). The evaluation of the tested molecules cytotoxicity on the HepG2 (hepatocarcinoma cell line purchased from ATCC, ref HB-8065) cell line was performed according to the method of Mosmann [36] with slight modifications. Briefly, 5 × 10³ cells in 100 mL of complete medium were inoculated into each well of 96-well plates and incubated at 37 °C in a humidified 6% CO₂. After 24 h incubation, 100 mL of medium with various product concentrations dissolved in DMSO (final concentration less than 0.5% v/v) were added and the plates were incubated for 72 h at 37 °C. Triplicate assays were performed for each sample. Each plate-well was then microscope-examined for detecting possible precipitate formation before the medium was aspirated from the wells. 100 mL of MTT (3-(4,5-dimethyl-2-thiazolyl)-2,5-diphenyl-2H-tetrazolium bromide) solution (0.5 mg/mL in medium without FCS) were then added to each well. Cells were incubated for 2 h at 37 °C. After this time, the MTT solution was removed and DMSO (100 mL) was added to dissolve the resulting blue formazan crystals. Plates were shaken vigorously (700 rpm) for 10 min. The absorbance was measured at 570 nm with 630 nm as reference wavelength using a BIO-TEK ELx808 Absorbance Microplate Reader. DMSO was used as blank and doxorubicin (purchased from Sigma Aldrich) as positive control. Cell viability was calculated as percentage of control (cells incubated without compound). The 50% cytotoxic concentration (CC₅₀) was determined from the dose–response curve by using the TableCurve 2D

v.5.0 software (Jandel scientific). CC_{50} values represent the mean value calculated from three independent experiments.

4.3.7. Cytotoxicity on THP-1 cell line

The evaluation of the tested molecules cytotoxicity on the THP-1 cell line (acute monocytic leukemia cell line purchased from ATCC, ref TIB-202) was performed according to the method of Mosman [36] with slight modifications. Briefly, cells in 100 μ L of complete RPMI medium, were incubated at an average density of 5×10^4 cells/mL in sterile 96-well plates with various concentrations of compounds dissolved in DMSO (final concentration less than 0.5% v/v), in duplicate. The plates were incubated for 72 h at 37 °C. Each well plate was then microscope-examined for detecting possible precipitate formation before the medium was aspirated from the wells. 100 μ L of MTT solution (0.5 mg/mL in medium without FCS) were then added to each well. Cells were incubated for 2 h at 37 °C. After this time, the MTT solution was removed and DMSO (100 μ L) was added to dissolve the resulting blue formazan crystals. Plates were shaken vigorously (300 rpm) for 10 min. The absorbance was measured at 570 nm with 630 nm as reference wavelength spectrophotometer using a BIO-TEK ELx808 Absorbance Microplate Reader. DMSO was used as blank and doxorubicin (purchased from Sigma Aldrich) as positive control. Cell viability was calculated as percentage of control (cells incubated without compound). The 50% cytotoxic concentration (CC_{50}) was determined from the dose–response curve by using the TableCurve 2D v.5.0 software. CC_{50} values represent the mean value calculated from three independent experiments.

4.3.8. Plasma protein binding

Plasma doped with the tested compound is incubated at 37 °C in triplicate in one of the compartments of the insert, the other compartment containing a phosphate buffer solution at pH

7.2. After stirring for 4 h at 300 rpm, a 25 μL aliquot of each compartment is taken and diluted; the dilution solution is adapted to obtain an identical matrix for all the compartments after dilution. In parallel, the reprocessing of a plasma doped but not incubated will allow to evaluate the recovery of the study. The LC-MS used for this study is a Waters[®] Acquity I-Class / Xevo TQD, equipped with a Waters[®] Acquity BEH C18 column, 50×2.1 mm, $1.7 \mu\text{M}$. The mobile phases are (A) ammonium acetate 10 mM and (B) acetonitrile with 0.1% formic acid. The injection volume is 1 μL and the flow rate is 600 $\mu\text{L}/\text{min}$. The chromatographic analysis, total duration of 4 min, is made with the following gradient: $0 < t < 0.2$ min, 2% (B); $0.2 < t < 2$ min, linear increase to 98% (B); $2 < t < 2.5$ min, 98% (B); $2.5 < t < 2.6$ min, linear decrease to 2% (B); $2.6 < t < 4$ min, 2% (B). Carbamazepine, oxazepam, warfarin and diclofenac are used as reference drugs and propranolol is used as internal standard. The unbound fraction (f_u) is calculated according to the following formula: $f_u = \frac{A_{\text{Plasma},4\text{h}} - A_{\text{PBS},4\text{h}}}{A_{\text{Plasma},4\text{h}}} \times 100$. The percentage of recovery is calculated according to the following formula:

$$\% \text{ Recovery} = \frac{(V_{\text{PBS}} \times A_{\text{PBS},4\text{h}}) + (V_{\text{Plasma}} \times A_{\text{Plasma},4\text{h}})}{(V_{\text{Plasma}} \times A_{\text{Plasma},0\text{h}})}$$

Where A is the ratio of the area under peak of the studied molecule and the area under peak of the internal standard (propranolol 200 nM). V is the volume of solution present in the compartments ($V_{\text{PBS}} = 350 \mu\text{L}$ and $V_{\text{plasma}} = 200 \mu\text{L}$).

4.3.9. Microsomal stability

The tested product and propranolol, used as reference, are incubated in duplicate (reaction volume of 0.5 mL) with female mouse microsomes (CD-1, 20 mg/mL, BD Gentest[™]) at 37 °C in a 50 mM phosphate buffer, pH 7.4, in the presence of MgCl_2 (5 mM), NADP (1 mM), glucose-6-phosphate dehydrogenase (0.4 U/mL) and glucose-6-phosphate (5 mM). For the estimation of the intrinsic clearance: 50 μL aliquot at 0, 5, 10, 20, 30 and 40 min are collected and the reaction is

stopped with 4 volumes of acetonitrile (ACN) containing the internal standard. After centrifugation at 10000 g, 10 min, 4 °C, the supernatants are kept at 4 °C for immediate analysis or placed at -80 °C in case of postponement of the analysis. Controls (t_0 and t_{final}) in triplicate are prepared by incubation of the internal standard with microsomes denatured by acetonitrile. The LC-MS used for this study is a Waters® Acquity I-Class / Xevo TQD, equipped with a Waters® Acquity BEH C18 column, 50 × 2.1 mm, 1.7 μm. The mobile phases are (A) ammonium acetate 10 mM and (B) acetonitrile with 0.1% formic acid. The injection volume is 1 μL and the flow rate is 600 μL/min. The chromatographic analysis, total duration of 4 min, is made with the following gradient: 0 < t < 0.2 min, 2% (B); 0.2 < t < 2 min, linear increase to 98% (B); 2 < t < 2.5 min, 98% (B); 2.5 < t < 2.6 min, linear decrease to 2% (B); 2.6 < t < 4 min, 2% (B). 8-Bromo-6-chloro-3-nitro-2-(phenylsulfonylmethyl)imidazo[1,2-*a*]pyridine **1c** is used as internal standard. The quantification of each compound is obtained by converting the average of the ratios of the analyte/internal standard surfaces to the percentage of consumed product. The ratio of the control at t_0 corresponds to 0% of product consumed. The calculation of the half-life ($t_{1/2}$) of each compound in the presence of microsomes is done according to the equation: $t_{1/2} = \frac{\ln(2)}{k}$, where k is the first-order degradation constant (the slope of the logarithm of compound concentration versus incubation time). The intrinsic clearance *in vitro* (Cl_{int} expressed in μL/min/mg) is calculated according to the equation:

$$Cl_{\text{int}} = \frac{\text{dose}}{AUC_{\infty}} / [\text{microsomes}]$$

Where dose is the initial concentration of product in the sample, AUC_{∞} is the area under the concentration-time curve extrapolated to infinity and [microsomes] is the microsome concentration expressed in mg/μL.

4.3.10. Parallel artificial membrane permeability assay (PAMPA)

The Pampa-BBB experiments were conducted using the Pampa Explorer Kit (Pion Inc) according to manufacturer's protocol. Briefly, the stock compound solution (20 mM in DMSO) was diluted in Prisma HT buffer pH 7.4 (pION) to 100 μ M. 200 μ L of this solution (n = 6) was added to donor plate (P/N 110243). 5 μ L of the BBB-1 Lipid (P/N 110672) was used to coat the membrane filter of the acceptor plate (P/N 110243). 200 μ L of the Brain Sink Buffer (P/N 110674) was added to each well of the acceptor plate. The sandwich was incubated at room temperature for 4 h, without stirring. After the incubation the UV-visible spectra were measured with the microplate reader (Tecan infinite M200) and the permeability value (P_e) was calculated by the PAMPA Explorer software v.3.7 (pION). Corticosterone ($P_e = 130.3 \pm 7.1$ nm/s), and theophylline ($P_e = 4.7 \pm 0.6$ nm/s) were used as high and low permeability standards, respectively. Each measure was performed in sixuplicate.

4.4. Thermodynamic solubility at pH 7.4 of compound 15

Thermodynamic solubility at pH 7.4 of compounds was determined according to a miniaturized shake-flask method (Organisation for Economic Cooperation and Development guideline n°105) [37]. Phosphate Buffer solutions (pH 7.4, 10 μ M, ionic strength 150 μ M) were prepared from Na_2HPO_4 , KH_2PO_4 and KCl (Sigma Aldrich, Saint Quentin Fallavier, France); 10 μ L of 20 mM stock solution were added to 5 mL glass tube containing 990 mL buffer (n = 4). Tubes were briefly sonicated and shaken by inversion during 24 h at room temperature. Then, tube contents were put in a microtube which was centrifuged at 12,225 g for 10 min; 100 μ L supernatant was mixed with 100 μ L acetonitrile in a Greiner UV microplate. Standard solutions were prepared extemporaneously diluting 20 mM DMSO stock solutions at 0, 2 and 5 mM; 5 μ L each working solution was diluted with 995 μ L buffer and 100 μ L was then mixed in microplate with 100 μ L acetonitrile to keep unchanged the final proportions of each solvent in standard solutions and samples. Determination of solubility at pH 7.4 was calculated from UV spectra (230 to 450 nm) obtained using a Synergy 2 (Biotek, Colmar, France) microplate reader. The calibration

curve was obtained from absorbance measures at 370 nm of the three standard solutions at 0, 10 and 25 μM in a 50:50 (vol/vol) mixture of buffer with acetonitrile/DMSO (99:1; vol/vol). Calibration curves were linear with $R^2 > 0.99$.

4.5. Micronucleus assay method

Cell line: the micronucleus assay was performed on a Chinese Hamster Ovary cell line CHO-K1 (ATCC, United States, ATCC[®] CCL-61, n^o6574112, Lot 12516, low passage number (<50).

Culture medium: McCoy's 5A medium (PAN BIOTECH, Lot 4487521) supplemented with 1 mM glutamine, 10 $\mu\text{g}/\text{mL}$ of a mixture of penicillin-streptomycin (PAN BIOTECH, Lot 784561) and 10% of inactivated calf serum (PAN BIOTECH, Lot P114526), pH 7.2, freshly prepared, stored no longer than 1 week.

Dilutions of test substances: the test material was dissolved into DMSO. Due to its low solubility in the culture medium, the maximal soluble concentration to be tested was 0.5 mM.

Controls: solvent control: PBS; Positive controls: mitomycin C (0.6 $\mu\text{g}/\text{mL}$) and benzo[*a*]pyrene (5 $\mu\text{g}/\text{mL}$), diluted in DMSO and stored at -80 °C.

Test procedure: all the assays were conducted in duplicate. The CHO-K1 cells, suspended in McCoy's 5A medium, were transferred into Labteck wells at a concentration of 100,000 cells/ml, and incubated for 24 h at 37°C in CO₂ (5%). When the test was performed without metabolic activation, the test substances were added into cell cultures at concentrations previously defined. A negative control containing culture medium, a solvent control containing 1% DMSO and a positive control containing 0.6 $\mu\text{g}/\text{mL}$ of mitomycin C were added. When the assay was performed in the presence of metabolic activation, S9 mix metabolizing mixture was added to cell cultures at a concentration of 10%. Then the test substances were added to the cell cultures at concentrations previously defined. A negative control containing culture medium, a solvent control containing 1% DMSO and a positive control containing 5 $\mu\text{g}/\text{ml}$ of benzo[*a*]pyrene were added. After 3 hours of incubation at 37 °C in CO₂ (5%), the culture medium was removed, the cells were rinsed with

phosphate buffered saline (PBS), and then returned to culture in McCoy's 5A medium containing 3 µg/ml of cytochalasin B. After a 21-hour incubation period at 37°C, cells were rinsed with phosphate buffered saline (PBS), fixed with methanol and stained with 10% Giemsa for 20 minutes.

Analysis of results: the analysis of results was performed under a microscope at ×1000 magnification. The antiproliferative activity of test substances was estimated by counting the number of binucleated cells relative to the number of mononucleated cells on a total of 500 cells for each dose (250 cells counted per well). The proliferation index (Cytokinesis Blocked Proliferative Index CBPI) was calculated using the following formula:

$$CBPI = (2 \times BI + MONO)/500$$

BI: number of binucleated cells

MONO: number of mononucleated cells

The cytostasis index (CI%), i.e. the percentage of cell replication inhibition, was calculated using the following formula:

$$CI\%: 100 - \{100 \times (CBPI_{\text{test material}} - 1)/(CBPI_{\text{solvent control}} - 1)\}$$

After this step, only the doses inducing a decrease of less than $55 \pm 5\%$ of CI% as compared to the negative control were taken into account for counting micronuclei. The rates of micronuclei were evaluated for the presence of independent nuclear core entities in 1000 binucleated cells per well, which corresponds to 2000 cells examined by test substance dose. Micronuclei were identified as small nuclei well differentiated from cell nucleus, stained in the same manner and having a diameter less than one third of that of the cell nucleus.

Micronuclei rates obtained for different doses of test substances were compared to the negative control by a χ^2 test. The assay was considered positive if:

- A dose-response relationship was obtained between the rate of micronuclei and the doses tested,

- At least one of these doses induced a statistically significant increase ($P < 0.05$) in the number of micronucleated cells as compared to the negative control.

4.6. Comet assay

4.6.1. Cell culture and treatment

The human hepatocarcinoma cell line HepG2 was obtained from the American Type Culture Collection (ATCC, ref. HB-8065). Cells were cultured in Eagle's Minimum Essential Medium (EMEM, ref. ATCC® 30-2003TM) supplemented with 10% heat-inactivated fetal bovine serum, 100 U/mL penicillin and 0.1 mg/mL streptomycin (all from Gibco). Cells were maintained at 37 °C in a humidified atmosphere with 5% CO₂. Cells were used in passage number 5-8.

Compound 8 was tested at 3 concentrations (5, 10 and 20 µM) for 3 different times of incubation (2, 24 and 72 h). Briefly, HepG2 cells were seeded at 1.13×10^5 cells/mL in 6-well plates (3 mL of cell suspension per well) and incubated at 37 °C in a humidified atmosphere with 5% CO₂. After 24, 72 and 94 h of incubation, cells were treated with different concentrations of the compound or the vehicle (0.5% dimethylsulfoxide, DMSO) for 72, 24 and 2 h respectively. Additionally, in the 2 h treatment plate, cell in an additional well were treated with 1mM methyl methanesulfonate (MMS) as positive control for the comet assay.

After treatment, medium was removed from the wells and cells were washed with phosphate buffered saline (PBS). Finally, cells were trypsinized and trypsin was neutralized with fresh medium. From this point, cells were kept ice-cold to avoid DNA repair.

4.6.2. Comet assay

The standard alkaline comet assay was employed for the detection of DNA strand breaks (SBs) and alkali-labile sites (ALS) in cell treated with compound 8. Trypsinized HepG2 cells were centrifuged at 125 g for 5 min at 4 °C and resuspended in cold PBS at 1×10^6 cells/mL. For the preparation of the agarose gels, 30 µL of cell suspension were mixed with 140 µL of 1 % low melting point agarose in PBS at 37 °C and 2 aliquots of 70 µL of cell/agarose mixture were placed

on agarose-precoated microscope slides. Each droplet was covered with a 20 x 20 mm coverslip and after 2-3 min on a cold metal plate the coverslips were removed. Then, slides were immersed in lysis solution (2.5 M NaCl, 0.1 M Na₂EDTA, 0.01 M Tris base, pH 10 and 1% Triton X-100) at 4 °C for 1 h. After lysis, slides were transferred to the electrophoresis tank and incubated for 40 min at 4 °C in the electrophoresis solution (0.3 M NaOH, 1 mM Na₂EDTA, pH > 13) to allow DNA unwinding. After that, electrophoresis was carried out at 1.2 V/cm for 20 min (4 °C). Then, gels were neutralized and washed by immersing the slides in PBS for 10 min and distilled water for another 10 min (both at 4 °C). Gels were then air dried at room temperature.

Comets were stained by adding 30 µL of 1 µg/mL of 4,6-diamidino-2-phenylindole (DAPI) on top of each gel and placing 22 x 22 mm coverslips on top. Slides were incubated with DAPI at room temperature for 30 mins before the analysis. The semi-automated image analysis system Comet Assay IV (Instem) was used to evaluate 50 comets per gel (100/condition). The percentage of DNA in tail was the descriptor used for each comet.

4.6.3. Statistics

The median percentage of DNA in tail for 50 comets was calculated for each of the duplicate gels in each experiment and the mean of the two medians was then calculated. The mean percentage of DNA in tail of 3 independent experiments and the standard deviation (SD) were calculated.

4.7. *In vivo* analysis

Female Swiss mice of 8 weeks (weight 30-32 g) are used. Mice were housed and procedures were conducted in agreement with european directive 2010/63/EU on animals used for scientific purposes applied in France as the 'Décret n°2012-118 du 1er février 2013 relatif à la protection des animaux utilisés à des fins scientifiques'. Accordingly, the present project was APAFIS#19730-2019031215178087 v1 authorized by the 'Ministère de l'Education Nationale, de l'Enseignement Supérieur et de la Recherche'.

The determination of maximal tolerated dose used one group of 4 mice which received an oral administration of **8** at 100 mg/kg. **8** was prepared as a suspension comprising 5% Tween 80/ 95% carboxymethylcellulose 0.5% in water.

Observations of side effects were codified. The same protocol was used with repeated dose during 5 days.

4.7.1. *In vivo* pharmacokinetics parameters

Chemicals: The internal standard (IS), ornidazole, was obtained from Sigma Aldrich. LC-MS Optima grade acetonitrile (ACN) and methanol (MeOH), acetic acid and formic acid (FA) were purchased from Fisher Scientific. Ready-to-use QuEChERS salts (6 g MgSO₄/1.5 g NaCl/1.5 g sodium citrate dihydrate/750 mg sodium citrate sesquihydrate) were supplied by VWR.

Sample preparation: samples were stored at -20 °C until extraction. 200 µL of ACN containing ornidazole (internal standard; IS) at a concentration of 62.5 ng/mL were added to 100 µL blood samples. The mixture was vortexed during 30 sec. After 10 min, 40 mg of QuEChERS salts were added. Samples were briefly vortexed and centrifuged at 16,000 g for 10 min. Ten microliters of the upper layer was directly transferred in an injection vial before being diluted (1/10; v/v) in a 0.1 % formic acid in water. Finally, 5 µL were injected in the LC-MS-MS system. Calibrations standards (9 levels, from 5 to 1,000 ng/mL) and quality controls (QC) (10, 75 and 625 ng/mL) were obtained by adding appropriate 20 × working standard solutions in blank whole blood.

LC-MS/MS conditions: the chromatographic system consisted in two Shimadzu LC-30 AD pumps (NexeraX2), a CTO 20AC oven, and a SIL-30AC autosampler (Shimadzu, Marne-la-Vallée, France). Chromatographic separation was performed using a EC-C8 column (Poroshell 120, 2.1 mm × 75 mm, 2.7 µM; Agilent) at a flow rate of 0.25 mL/min using a gradient of 0.1% acetic acid in water (A) and 0.1% acetic acid in MeOH/ACN 50:50 (B) programmed as follows: 0.0–0.1, 20% (B); 0.1–1.0, 20 to 70% (B); 1.0–4.0, 70% to 100% (B); 4.0–5.5, 100% (B); 5.5–6.0,

100 to 20% (B); and 6.0–8.0 column equilibration with 20% (B). Oven temperature was set at 60 °C.

A Shimadzu 8060 triple quadrupole mass spectrometer was used in the positive electrospray ionization mode. The main common parameter settings were as follows: interface voltage, 1.5 kV; nebulizing gas flow, 3 L/min; heating gas flow, 10 L/min; interface temperature, 300 °C; desolvation line (DL) temperature, 250 °C; heat block temperature, 400 °C; and drying gas flow, 10 L/min. All parameters (collision energy, Q1/Q3 pre-bias) were optimized from standard flow injection analysis. Dwell time was set at 100 ms per transition.

Validation procedure for whole blood: validation protocol and the set of acceptance criteria were as follows:

- Linearity: Calibration curve was generated by plotting the peak area ratios (analyte/internal standard) vs the expected concentration. Linearity of the calibration curve was evaluated by a quadratic regression analysis using a $1/x^2$ weighting. A value greater than 0.99 was expected for the coefficient of determination (r^2).
- Precision and accuracy of the method were assessed at lower limit of quantitation (LLOQ; 5 ng/mL) and at the three quality control concentrations (10, 75 and 625 ng/mL). Precision is calculated as the coefficient of variation (CV%) within a single run (intra-assay; $n = 5$) and between different assays (inter-assay; $n = 5$), and accuracy is the percentage of deviation between nominal and found concentration with the established calibration curve. Acceptance criteria were intra-assay and inter-assay precision (CV%) and an accuracy (bias) less than 20%.
- The lower limit of quantification (LLOQ) was estimated to be the minimal concentration with accuracy and precision within $\pm 20\%$. The lower limit of detection (LLOD) was calculated based on a signal-to-noise ratio >3 .

- Extraction recoveries were determined by comparing the LLOQ and the quality controls samples (n = 5) with their extracted blank whole blood counterparts spiked at the correct concentration after extraction (n = 3). CV% in the extraction recovery had to be less than 20%.
- The effect of dilution was investigated on samples spiked at MQC and HQC then analyzed after 1.25-, two- and four-fold dilutions and on samples spiked at 150% of ULOQ (1500 ng/ml) for a two-fold dilution. Precision CV and bias were set less than 25% to successfully validate.
- The absence of carryover was checked by injecting blank samples just after the analysis of the most concentrated sample (1,000 ng/mL).

Pharmacokinetics: the same samples used for the validation were used for the analysis. Monolix Lixoft software was used to analyze data by noncompartmental model to fit pharmacokinetics parameters.

Acknowledgement

This work is supported by Aix-Marseille Université, the Université de Toulouse and the CNRS. A. Fairlamb and S. Wyllie are supported by funding from the Wellcome Trust (WT105021). C. Fersing thanks the Assistance Publique - Hôpitaux de Marseille (AP-HM) for hospital appointment. J. Pedron thanks the Université Paul Sabatier and the Conseil Régional Occitanie for PhD funding. The authors thank Dr Vincent Remusat for the NMR spectra recording, Dr Christophe Chendo and Dr Valérie Monnier for the HRMS analyses. Catherine Piveteau and Alexandre Biela from Institut Pasteur de Lille are also acknowledged for their contribution in determining *in vitro* PK parameters. We thank Dr Jean-Baptiste Woillard for the *in vivo* pharmacokinetic analysis and Mr François-Ludovic Sauvage for his help in mass spectrometry analysis. Dr. Amaya Azqueta thanks the 'Ramon y Cajal' programme (RYC-2013-14370) of the Spanish Government.

References

- [1] D.H. Molyneux, L. Savioli, D. Engels, Neglected tropical diseases: progress towards addressing the chronic pandemic, *Lancet Lond. Engl.* 389 (2017) 312–325. [https://doi.org/10.1016/S0140-6736\(16\)30171-4](https://doi.org/10.1016/S0140-6736(16)30171-4).
- [2] S.P.S. Rao, M.P. Barrett, G. Dranoff, C.J. Faraday, C.R. Gimpelewicz, A. Hailu, C.L. Jones, J.M. Kelly, J.K. Lazdins-Helds, P. Mäser, J. Mengel, J.C. Mottram, C.E. Mowbray, D.L. Sacks, P. Scott, G.F. Späth, R.L. Tarleton, J.M. Spector, T.T. Diagana, Drug Discovery for Kinetoplastid Diseases: Future Directions, *ACS Infect. Dis.* 5 (2019) 152–157. <https://doi.org/10.1021/acsinfecdis.8b00298>.
- [3] WHO | 10th meeting of the Strategic and Technical Advisory Group for Neglected Tropical Diseases, WHO. (n.d.). http://www.who.int/neglected_diseases/events/tenth_stag/en/ (accessed June 4, 2019).
- [4] S. Burza, S.L. Croft, M. Boelaert, Leishmaniasis, *Lancet Lond. Engl.* 392 (2018) 951–970. [https://doi.org/10.1016/S0140-6736\(18\)31204-2](https://doi.org/10.1016/S0140-6736(18)31204-2).
- [5] J.A. Pérez-Molina, I. Molina, Chagas disease, *Lancet Lond. Engl.* 391 (2018) 82–94. [https://doi.org/10.1016/S0140-6736\(17\)31612-4](https://doi.org/10.1016/S0140-6736(17)31612-4).
- [6] P. Büscher, G. Cecchi, V. Jamonneau, G. Priotto, Human African trypanosomiasis, *Lancet Lond. Engl.* (2017). [https://doi.org/10.1016/S0140-6736\(17\)31510-6](https://doi.org/10.1016/S0140-6736(17)31510-6).
- [7] P.G.E. Kennedy, Update on human African trypanosomiasis (sleeping sickness), *J. Neurol.* 266 (2019) 2334–2337. <https://doi.org/10.1007/s00415-019-09425-7>.
- [8] J.R. Franco, G. Cecchi, G. Priotto, M. Paone, A. Diarra, L. Grout, P.P. Simarro, W. Zhao, D. Argaw, Monitoring the elimination of human African trypanosomiasis: Update to 2016, *PLoS Negl. Trop. Dis.* 12 (2018) e0006890. <https://doi.org/10.1371/journal.pntd.0006890>.
- [9] E.A. Dickie, F. Giordani, M.K. Gould, P. Mäser, C. Burri, J.C. Mottram, S.P.S. Rao, M.P. Barrett, New Drugs for Human African Trypanosomiasis: A Twenty First Century Success Story, *Trop. Med. Infect. Dis.* 5 (2020). <https://doi.org/10.3390/tropicalmed5010029>.
- [10] About Sleeping Sickness | DNDi, Drugs Neglected Dis. Initiat. DNDi. (n.d.). <https://www.dndi.org/diseases-projects/hat/> (accessed April 9, 2019).
- [11] E.D. Deeks, Fexinidazole: First Global Approval, *Drugs.* 79 (2019) 215–220. <https://doi.org/10.1007/s40265-019-1051-6>.

- [12] S. Patterson, S. Wyllie, Nitro drugs for the treatment of trypanosomatid diseases: past, present, and future prospects, *Trends Parasitol.* 30 (2014) 289–298. <https://doi.org/10.1016/j.pt.2014.04.003>.
- [13] B. S. Hall, C. Bot, S. R. Wilkinson, Nifurtimox Activation by Trypanosomal Type I Nitroreductases Generates Cytotoxic Nitrile Metabolites, *J. Biol. Chem.* 15 (2011) 13088–13095. <https://doi.org/10.1074/jbc.M111.230847>.
- [14] K. Nepali, H. Y. Lee, J-P. Liou, Nitro-Group-Containing Drugs, *J. Med. Chem.* 62 (2019) 2851–2893. <https://doi.org/10.1021/acs.jmedchem.8b00147>.
- [15] C. Castera-Ducros, L. Paloque, P. Verhaeghe, M. Casanova, C. Cantelli, S. Hutter, F. Tanguy, M. Laget, V. Remusat, A. Cohen, M.D. Crozet, P. Rathelot, N. Azas, P. Vanelle, Targeting the human parasite *Leishmania donovani*: Discovery of a new promising anti-infectious pharmacophore in 3-nitroimidazo[1,2-a]pyridine series, *Bioorg. Med. Chem.* 21 (2013) 7155–7164. <https://doi.org/10.1016/j.bmc.2013.09.002>.
- [16] C. Fersing, L. Basmaciyan, C. Boudot, J. Pedron, S. Hutter, A. Cohen, C. Castera-Ducros, N. Primas, M. Laget, M. Casanova, S. Bourgeade-Delmas, M. Piednoel, A. Sournia-Saquet, V. Belle Mbou, B. Courtioux, É. Boutet-Robinet, M. Since, R. Milne, S. Wyllie, A.H. Fairlamb, A. Valentin, P. Rathelot, P. Verhaeghe, P. Vanelle, N. Azas, Nongenotoxic 3-Nitroimidazo[1,2-a]pyridines Are NTR1 Substrates That Display Potent in Vitro Antileishmanial Activity, *ACS Med. Chem. Lett.* 10 (2019) 34–39. <https://doi.org/10.1021/acsmchemlett.8b00347>.
- [17] C. Fersing, C. Boudot, J. Pedron, S. Hutter, N. Primas, C. Castera-Ducros, S. Bourgeade-Delmas, A. Sournia-Saquet, A. Moreau, A. Cohen, J.-L. Stigliani, G. Pratviel, M.D. Crozet, S. Wyllie, A. Fairlamb, A. Valentin, P. Rathelot, N. Azas, B. Courtioux, P. Verhaeghe, P. Vanelle, 8-Aryl-6-chloro-3-nitro-2-(phenylsulfonylmethyl)imidazo[1,2-a]pyridines as potent antitrypanosomatid molecules bioactivated by type 1 nitroreductases, *Eur. J. Med. Chem.* 157 (2018) 115–126. <https://doi.org/10.1016/j.ejmech.2018.07.064>.
- [18] C. Castera, M. D. Crozet, P. Vanelle, An Efficient Synthetic Route to New Imidazo[1,2-a]pyridines by Cross-Coupling Reactions in Aqueous Medium, *HETEROCYCLES.* 65 (2005) 2979–2989. <https://doi.org/10.3987/COM-05-10548>.
- [19] M.D. Crozet, C. Castera-Ducros, P. Vanelle, An efficient microwave-assisted Suzuki cross-coupling reaction of imidazo[1,2-a]pyridines in aqueous medium, *Tetrahedron Lett.* 47 (2006) 7061–7065. <https://doi.org/10.1016/j.tetlet.2006.07.098>.

- [20] L.G. Menchikov, A.V. Vorogushin, O.S. Korneva, O.M. Nefedov, An Effective Method for Alcohol Preparation by Hydrolysis of Organohalides in the Presence of Copper and its Salts in Aqueous DMSO, *Mendeleev Commun.* 5 (1995) 223–224. <https://doi.org/10.1070/MC1995v005n06ABEH000536>.
- [21] M.D. Crozet, C. Castera, M. Kaafarani, M.P. Crozet, P. Vanelle, Synthesis of new 6-halogeno-imidazo[1,2-a]pyridines by SRN1 reactions, *Arkivoc.* 2003 (2003) 273–282. <https://doi.org/10.3998/ark.5550190.0004.a26>.
- [22] P. Verhaeghe, A. Dumètre, C. Castera-Ducros, S. Hutter, M. Laget, C. Fersing, M. Prieri, J. Yzombard, F. Sifredi, S. Rault, P. Rathelot, P. Vanelle, N. Azas, 4-Thiophenoxy-2-trichloromethyquinazolines display in vitro selective antiplasmodial activity against the human malaria parasite *Plasmodium falciparum*, *Bioorg. Med. Chem. Lett.* 21 (2011) 6003–6006. <https://doi.org/10.1016/j.bmcl.2011.06.113>.
- [23] C. Kieffer, A. Cohen, P. Verhaeghe, S. Hutter, C. Castera-Ducros, M. Laget, V. Remusat, M.K. M'Rabet, S. Rault, P. Rathelot, N. Azas, P. Vanelle, Looking for new antileishmanial derivatives in 8-nitroquinolin-2(1H)-one series, *Eur. J. Med. Chem.* 92 (2015) 282–294. <https://doi.org/10.1016/j.ejmech.2014.12.056>.
- [24] D. Singh, A.M. Deobald, L.R.S. Camargo, G. Tabarelli, O.E.D. Rodrigues, A.L. Braga, An Efficient One-Pot Synthesis of Symmetrical Diselenides or Ditellurides from Halides with CuO Nanopowder/Se⁰ or Te⁰/Base, *Org. Lett.* 12 (2010) 3288–3291. <https://doi.org/10.1021/ol100558b>.
- [25] J. McCann, N.E. Spingarn, J. Kabori, B.N. Ames, Detection of carcinogens as mutagens: bacterial tester strains with R factor plasmids., *Proc. Natl. Acad. Sci.* 72 (1975) 979–983. <https://doi.org/10.1073/pnas.72.3.979>.
- [26] D. Tweats, B. Bourdin Trunz, E. Torreele, Genotoxicity profile of fexinidazole--a drug candidate in clinical development for human African trypanomiasis (sleeping sickness), *Mutagenesis.* 27 (2012) 523–532. <https://doi.org/10.1093/mutage/ges015>.
- [27] OECD, Test No. 471: Bacterial Reverse Mutation Test, OECD, 1997. <https://doi.org/10.1787/9789264071247-en>.
- [28] T.T. Wager, X. Hou, P.R. Verhoest, A. Villalobos, Moving beyond Rules: The Development of a Central Nervous System Multiparameter Optimization (CNS MPO) Approach To Enable Alignment of Druglike Properties, *ACS Chem. Neurosci.* 1 (2010) 435–449. <https://doi.org/10.1021/cn100008c>.

- [29] C. Zhang, S. Bourgeade Delmas, Á. Fernández Álvarez, A. Valentin, C. Hemmert, H. Gornitzka, Synthesis, characterization, and antileishmanial activity of neutral N-heterocyclic carbenes gold(I) complexes, *Eur. J. Med. Chem.* 143 (2018) 1635–1643. <https://doi.org/10.1016/j.ejmech.2017.10.060>.
- [30] R. Inocência da Luz, M. Vermeersch, J.-C. Dujardin, P. Cos, L. Maes, In Vitro Sensitivity Testing of Leishmania Clinical Field Isolates: Preconditioning of Promastigotes Enhances Infectivity for Macrophage Host Cells, *Antimicrob. Agents Chemother.* 53 (2009) 5197–5203. <https://doi.org/10.1128/AAC.00866-09>.
- [31] B. Ráz, M. Iten, Y. Grether-Bühler, R. Kaminsky, R. Brun, The Alamar Blue® assay to determine drug sensitivity of African trypanosomes (*T.b. rhodesiense* and *T.b. gambiense*) in vitro, *Acta Trop.* 68 (1997) 139–147. [https://doi.org/10.1016/S0001-706X\(97\)00079-X](https://doi.org/10.1016/S0001-706X(97)00079-X).
- [32] T. Baltz, D. Baltz, C. Giroud, J. Crockett, Cultivation in a semi-defined medium of animal infective forms of *Trypanosoma brucei*, *T. equiperdum*, *T. evansi*, *T. rhodesiense* and *T. gambiense*., *EMBO J.* 4 (1985) 1273–1277. <https://doi.org/10.1002/j.1460-2075.1985.tb03772.x>.
- [33] N. Greig, S. Wyllie, S. Patterson, A.H. Fairlamb, A comparative study of methylglyoxal metabolism in trypanosomatids: Methylglyoxal metabolism in trypanosomatids, *FEBS J.* 276 (2009) 376–386. <https://doi.org/10.1111/j.1742-4658.2008.06788.x>.
- [34] S. Wyllie, B.J. Foth, A. Kelner, A.Y. Sokolova, M. Berriman, A.H. Fairlamb, Nitroheterocyclic drug resistance mechanisms in *Trypanosoma brucei*, *J. Antimicrob. Chemother.* 71 (2016) 625–634. <https://doi.org/10.1093/jac/dkv376>.
- [35] D.C. Jones, I. Hallyburton, L. Stojanovski, K.D. Read, J.A. Frearson, A.H. Fairlamb, Identification of a κ -opioid agonist as a potent and selective lead for drug development against human African trypanosomiasis, *Biochem. Pharmacol.* 80 (2010) 1478–1486. <https://doi.org/10.1016/j.bcp.2010.07.038>.
- [36] T. Mosmann, Rapid colorimetric assay for cellular growth and survival: Application to proliferation and cytotoxicity assays, *J. Immunol. Methods.* 65 (1983) 55–63. [https://doi.org/10.1016/0022-1759\(83\)90303-4](https://doi.org/10.1016/0022-1759(83)90303-4).
- [37] C. Lecoutey, D. Hedou, T. Freret, P. Giannoni, F. Gaven, M. Since, V. Bouet, C. Ballandonne, S. Corvaisier, A. Malzert Freon, S. Mignani, T. Cresteil, M. Boulouard, S. Claeysen, C. Rochais, P. Dallemagne, Design of donecopride, a dual serotonin subtype 4 receptor agonist/acetylcholinesterase inhibitor with potential interest for Alzheimer’s disease treatment, *Proc. Natl. Acad. Sci.* 111 (2014) E3825–E3830. <https://doi.org/10.1073/pnas.1410315111>.